N63 19471

NASA TR R-107

36379
30p

NATIONAL AERONAUTICS AND SPACE ADMINISTRATION

TECHNICAL REPORT
R-107

SIMILARITY SOLUTIONS FOR SMALL CROSS FLOWS IN LAMINAR COMPRESSIBLE BOUNDARY LAYERS

By IVAN E. BECKWITH

1961

30

CASE FILE COPY

ERRATA

NASA Technical Report R-107

SIMILARITY SOLUTIONS FOR SMALL CROSS FLOWS IN LAMINAR COMPRESSIBLE BOUNDARY LAYERS

By Ivan E. Beckwith
1961

Page 16, col. 2:

In equation (74) the first parenthesized term $\left(\frac{\bar{u}_e}{\bar{u}_e}\right)^2$ should be $\left(\frac{u_e}{\bar{u}_e}\right)^2$.

The second line after equation (74) should be corrected to read as follows:

(53), (68), and (73) into equation (47) where from

The second line after equation (75) should be corrected to read as follows:

Substituting equation (74) into equation (50)

Page 18, col. 1, eq. (85):

The first term after the equality sign should be corrected as follows:

$$\frac{1}{\bar{\beta}\lambda}$$

NASA-Langley, 1963

Issued 4-24-63

TECHNICAL REPORT R-107

SIMILARITY SOLUTIONS FOR SMALL CROSS FLOWS IN LAMINAR COMPRESSIBLE BOUNDARY LAYERS

By IVAN E. BECKWITH

Langley Research Center
Langley Field, Va.

TECHNICAL REPORT R-107

SIMILARITY SOLUTIONS FOR SMALL CROSS FLOWS IN LAMINAR COMPRESSIBLE BOUNDARY LAYERS

By IVAN E. BECKWITH

SUMMARY

The compressible laminar boundary-layer equations for an arbitrary three-dimensional body are reduced to a form analogous to the corresponding equations for axisymmetric flow. This simplification results from the use of a streamline coordinate system and the assumption that the component of boundary-layer flow normal to the external streamline (cross flow) is small. The streamwise skin friction and heat-transfer distributions on the arbitrary body are then independent of the cross flow. Formulas for computing these distributions are adapted from a local similarity method originally derived for a body of revolution.

The cross-flow momentum equation is simplified by a similarity transformation, and solutions are obtained for a large range of input conditions as represented by similarity parameters. General criteria that determine the limiting conditions for the valid assumption of small cross-flow are evaluated from these solutions. The cross-flow velocity and the limiting criteria both depend on the ratio of the crosswise pressure gradient to the streamwise pressure gradient.

The small-cross-flow theory is used to compute velocity profiles, skin friction, and heat transfer on a yawed circular cylinder. The results are compared with exact values obtained from local similarity solutions for the yawed infinite cylinder. These comparisons indicate that the assumption of small cross flow should give better predictions of friction and heating distributions for a larger range of body shapes, wall temperatures, and stream conditions than previously considered possible.

INTRODUCTION

Calculating heat transfer and skin friction on arbitrary three-dimensional bodies in high-speed flows is of increasing technical importance because of the reentry problem of lifting space vehicles. The complexity of the governing differential equations makes the use of simplifying approximations desirable so that tractable solutions may be obtained.

A very substantial simplification is obtained if the cross flow, that is, the component of boundary-layer flow normal to the direction of the local free-stream flow, is assumed small. Reference 1 showed that for the laminar boundary layer this assumption linearized the cross-flow momentum equation and that with additional assumptions for the metric coefficients, the coutinuity, energy, and streamwise momentum equations could be reduced to a two-dimensional form. In reference 2 it was shown that the assumption of small cross flow reduced the incompressible boundary-layer equations to a form analogous to the axisymmetric equations. In reference 3 it was pointed out that a similar result holds for compressible flows and further that the energy and streamwise momentum equations are independent of the cross-flow velocity. This independence implies that the heat transfer and streamwise shear can be computed as if the cross flow did not exist. After this computation is performed, the cross flow is then obtained from a linear equation.

Approximate integral methods for computing incompressible boundary layers with small cross flow are presented in references 3 to 5. In reference 6 the assumption of zero cross flow is shown to be applicable to highly cooled blunt bodies in hypersonic flow. The resulting equation for the heat transfer along inviscid streamlines is analogous to the corresponding equation for the axisymmetric case. (See ref. 7.)

This paper presents a discussion of the three-dimensional compressible laminar boundary layer with small but finite cross flow. The cross-flow momentum equation is reduced to an ordinary differential equation when similarity in a cross-flow velocity function is assumed. Solutions to this equation result in general criteria for the valid application of the small-cross-flow assumption. By application of local similarity as used in references 8 and 9, general equations for the heat-transfer distributions and skin friction along inviscid streamlines are derived. Application of these equations requires the pressure distribution along the streamlines and the normal spacing between them. The absolute level of heating is established from the appropriate exact solutions for stagnation flows as given in reference 10.

Streamwise skin friction and heat-transfer distributions computed by the present method are compared to the "exact" values on a yawed infinite cylinder from the local similarity method of reference 9. The cross-flow velocity profiles and skin friction from the small-cross-flow theory are also compared to the exact values. Consideration of the small-cross-flow criteria for the yawed cylinder makes possible some general conclusions regarding the effect of cross flow on heating and skin friction.

SYMBOLS

C	mass concentration
c	constant
c_p	frozen specific heat at constant pressure
D	binary diffusion coefficient
e_1, e_2	metric coefficients in curvilinear coordinate system defined by equations (1)
F	diffusion function, equation (8)
f	similar stream function, equation (21)
$f'=u/u_e$	
$\bar{f}'$	chordwise velocity ratio on yawed infinite cylinder, $\bar{u}/\bar{u}_e$
G	function of s, equation (27)
$\bar{g}$	spanwise velocity ratio on yawed infinite cylinder, $\bar{v}/\bar{v}_e$
H	stagnation enthalpy, $h+\frac{u^2+v^2}{2}$
h	static enthalpy
K	geodesic curvature of streamlines
k	frozen thermal conductivity
N_{Le}	Lewis number, $\rho c_p D/k$
n	distance normal to streamlines
p	pressure
P, Q, R, N	parameters in correlation function for $\theta'_w/\theta'_{w,\beta=1}$
N_{Pr}	frozen Prandtl number, $\mu c_p/k$
q	heat-transfer rate per unit area
R^*	radius of curvature of an arbitrary body at the stagnation point
r	radius of circular cylinder
s	distance along external inviscid streamlines projected on the body surface
t	enthalpy ratio, h/H_e
u, v, w	velocities in curvilinear coordinate directions
$\bar{u}, \bar{v}$	velocity components in Cartesian coordinate directions on yawed infinite cylinder
V	cross-flow velocity function, equation (26)
x, y, z	curvilinear coordinates as defined in sketch on page 3
$\bar{x}, \bar{y}$	chordwise and spanwise Cartesian coordinates for yawed infinite cylinder (see ref. 11)
α	angle between resultant velocity and cylinder generators
β	similarity parameter, equation (34) or equation (52)
β^*	similarity parameter, equation (35) or equation (51)
$\bar{\beta}$	similarity parameter for yawed infinite cylinder, equation (72)
γ	ratio of specific heats, 1.40 for air
ζ	stagnation enthalpy ratio, H/H_e
θ	enthalpy difference ratio, $\frac{H-H_w}{H_e-H_w}=\frac{\zeta-t_w}{1-t_w}$
θ^*_{tr}	transformed momentum thickness, $\int_0^\infty f'(1-f')d\eta$
Λ	yaw angle
λ	yaw parameter, $\frac{1}{1-(\bar{v}_\infty^2/2H_e)}$
μ	viscosity coefficient
ξ, η	similarity coordinates in streamline system, equations (19)
$\bar{\xi}$	function of ξ
ρ	mass density

τ	wall shear
τ_x	shear stress in streamwise direction
τ_y	shear stress in cross-flow direction
φ	density-viscosity product ratio, $\rho\mu/(\rho\mu)_w$
ψ	stream function, equations (20)
Subscripts:	
aw	adiabatic wall
e	local value external to boundary layer
i	ith species of gas mixture
max	maximum
min	minimum
o	reference point on body
s	stagnation region on yawed infinite cylinder where $\overline{u}_e=c\overline{x}$ and $p_e\approx$ Constant
sp	stagnation point
w	surface ($z=0$)
∞	ahead of bow shock

A superscript bar refers to quantities on yawed infinite cylinder unless otherwise noted. A prime indicates differentiation with respect to η.

GENERAL EQUATIONS

INTRINSIC COORDINATE SYSTEM

The Prandtl boundary-layer equations are written in terms of a three-dimensional, orthogonal, curvilinear coordinate system which is specialized to a streamline system intrinsic to the particular body or flow which is investigated. As illustrated in the following sketch the coordinate direction x

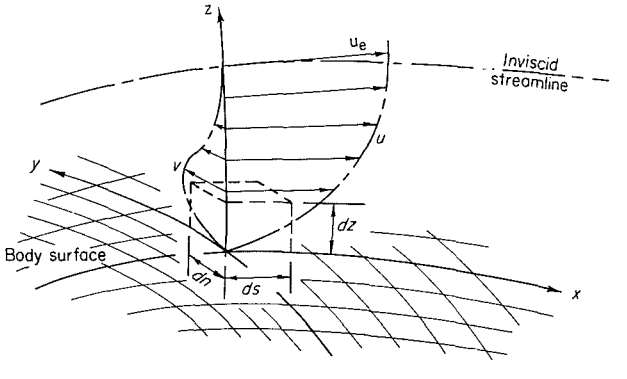

coincides with the local external inviscid streamline projected in the plane tangent to the surface; y is also in the tangent plane and normal to x; and z is normal to the tangent plane. The corresponding velocities are u, v, and w so that the velocities at the "edge" of the boundary layer are $u=u_e$ and $v=v_e=0$. The elements of length in the three coordinate directions are assumed to be

$$\left.\begin{aligned} ds&=e_1(x,y)\,dx\\ dn&=e_2(x,y)dy\\ dz&=dz \end{aligned}\right\} \tag{1}$$

which are consistent with the other Prandtl boundary-layer assumptions. (See refs. 3 and 12, for example.)

The boundary-layer equations may then be written as (refs. 1, 3, and 12)

Continuity:

$$\frac{1}{e_1}\frac{\partial}{\partial x}(\rho u e_2)+\frac{1}{e_1}\frac{\partial}{\partial y}(\rho v e_1)+\frac{\partial}{\partial z}(\rho w e_2)=0 \tag{2}$$

x-momentum:

$$\frac{\rho u}{e_1}\frac{\partial u}{\partial x}+\frac{\rho v}{e_2}\frac{\partial u}{\partial y}+\rho w\frac{\partial u}{\partial z}+\frac{\rho u v}{e_1 e_2}\frac{\partial e_1}{\partial y}-\frac{\rho v^2}{e_1 e_2}\frac{\partial e_2}{\partial x}=-\frac{1}{e_1}\frac{\partial p}{\partial x}+\frac{\partial}{\partial z}\left(\mu\frac{\partial u}{\partial z}\right) \tag{3}$$

y-momentum:

$$\frac{\rho u}{e_1}\frac{\partial v}{\partial x}+\frac{\rho v}{e_2}\frac{\partial v}{\partial y}+\rho w\frac{\partial v}{\partial z}+\frac{\rho u v}{e_1 e_2}\frac{\partial e_2}{\partial x}-\frac{\rho u^2}{e_1 e_2}\frac{\partial e_1}{\partial y}=-\frac{1}{e_2}\frac{\partial p}{\partial y}+\frac{\partial}{\partial z}\left(\mu\frac{\partial v}{\partial z}\right) \tag{4}$$

z-momentum:

$$\frac{\partial p}{\partial z}=0 \tag{5}$$

Energy:

$$\frac{\rho u}{e_1}\frac{\partial H}{\partial x}+\frac{\rho v}{e_2}\frac{\partial H}{\partial y}+\rho w\frac{\partial H}{\partial z}=\frac{\partial}{\partial z}\left[\mu\left(\frac{\partial H}{\partial z}+\frac{1-N_{Pr}+F}{N_{Pr}}\frac{\partial h}{\partial z}\right)\right] \tag{6}$$

where the gas is assumed in chemical equilibrium. The stagnation enthalpy H is defined as

$$H=h+\frac{u^2+v^2}{2} \tag{7}$$

and F is a diffusion function approximated for a binary mixture as

$$F=(N_{Le}-1)\sum h_i\left(\frac{\partial C_i}{\partial h}\right)_p \tag{8}$$

which is computed and tabulated for air in reference 13. The boundary conditions for equations (2) to (6) for all values of x and y are

$$\left.\begin{aligned} u(0)&=v(0)=0 \\ w(0)&=w_w \\ H(0)&=H_w=h_w \\ u(\infty)&=u_e \\ v(\infty)&=v_e=0 \\ H(\infty)&=H_e=h_e+\frac{u_e^2}{2} \end{aligned}\right\} \tag{9}$$

At the edge of the boundary layer (where $z\to\infty$) the derivatives of any quantity with respect to z are neglected, and since $v_e=0$ equations (3) and (4) reduce to

$$\frac{\rho_e u_e}{e_1}\frac{\partial u_e}{\partial x}=-\frac{1}{e_1}\frac{\partial p}{\partial x} \tag{10}$$

$$\frac{\rho_e u_e^2}{e_1 e_2}\frac{\partial e_1}{\partial y}=\frac{1}{e_2}\frac{\partial p}{\partial y} \tag{11}$$

where, on account of equation (5), $p=p_e$. Substituting the cross-flow pressure gradient from equation (11) into equation (4) then gives

$$\frac{\rho u}{e_1}\frac{\partial v}{\partial x}+\frac{\rho v}{e_2}\frac{\partial v}{\partial y}+\rho w\frac{\partial v}{\partial z}+\frac{\rho u v}{e_1 e_2}\frac{\partial e_2}{\partial x}=\frac{\rho u_e^2}{e_1 e_2}\frac{\partial e_1}{\partial y}\left[\left(\frac{u}{u_e}\right)^2-\frac{\rho_e}{\rho}\right]+\frac{\partial}{\partial z}\left(\mu\frac{\partial v}{\partial z}\right) \tag{12}$$

The quantity

$$\frac{1}{e_1 e_2}\frac{\partial e_1}{\partial y}$$

hereafter designated as K, is the local curvature of the plane curve obtained by projecting the inviscid streamline on the tangent plane.

SMALL CROSS FLOW

When the curvature of the streamlines is zero the first term on the right-hand side of equation (12) drops out and if the initial condition is $v(x_o,y_o,z)=0$ then the solution for v is $v=0$ since $v_w=v_e=0$. Thus, it would be expected that when the streamline curvature K is everywhere small the cross-flow velocity v is small. Reference 6 shows that v would also be small when the quantity

$$\left[\left(\frac{u}{u_e}\right)^2-\frac{\rho_e}{\rho}\right]$$

in equation (12) is small as is the case on the forward part of highly cooled blunt bodies.

The assumption of small but finite cross flow is introduced by neglecting higher order terms in v, K, and the lateral derivatives $\partial/\partial y$. (See ref. 3.) Furthermore, in accordance with equations (1), s is defined as the distance along an external inviscid streamline projected on the body surface; that is,

$$s=\int_0^x e_1\,dx$$

Equations (2), (3), (12), and (6) then become

$$\frac{\partial}{\partial s}(\rho u e_2)+\frac{\partial}{\partial z}(\rho w e_2)=0 \tag{13}$$

$$\rho u\frac{\partial u}{\partial s}+\rho w\frac{\partial u}{\partial z}=\rho_e u_e\frac{\partial u_e}{\partial s}+\frac{\partial}{\partial z}\left(\mu\frac{\partial u}{\partial z}\right) \tag{14}$$

$$\rho u\frac{\partial v}{\partial s}+\rho w\frac{\partial v}{\partial z}+\frac{\rho u v}{e_2}\frac{\partial e_2}{\partial s}=\rho u_e^2 K\left[\left(\frac{u}{u_e}\right)^2-\frac{\rho_e}{\rho}\right]+\frac{\partial}{\partial z}\left(\mu\frac{\partial v}{\partial z}\right) \tag{15}$$

$$\rho u\frac{\partial H}{\partial s}+\rho w\frac{\partial H}{\partial z}=\frac{\partial}{\partial z}\left[\mu\left(\frac{\partial H}{\partial z}+\frac{1-N_{Pr}+F}{N_{Pr}}\frac{\partial h}{\partial z}\right)\right] \tag{16}$$

where now

$$H=h+\frac{u^2}{2} \tag{17}$$

since $v^2/u^2\ll 1.0$.

Equations (13), (14), and (16) are independent of v and are of the same form as the corresponding equations for an axisymmetric body. (See ref. 3.) Therefore, if the distribution of pressure and the quantity e_2 are known along any particular streamline, the heat transfer and streamwise skin friction may be calculated along that streamline by any method applicable to a body of revolution. In this calculation the quantity e_2 would replace the radius of the body of revolution, and if each streamline is considered as a separate problem, both e_2 and p become, in effect, functions of s only. Presumably the values of ρ, u, and w could be computed in the same manner; then the corresponding values of v could be determined

from equation (15) which is linear.

Equation (15) may be written in a more convenient form by combining the first and third terms and noting that e_2 is independent of z. The result is

$$\rho u\frac{\partial}{\partial s}(e_2v)+\rho w\frac{\partial}{\partial z}(e_2v)=\rho u_e^2e_2K\left[\left(\frac{u}{u_e}\right)^2-\frac{\rho_e}{\rho}\right]+\frac{\partial}{\partial z}\left[\mu\frac{\partial}{\partial z}(e_2v)\right] \quad (18)$$

SIMILAR EQUATIONS FOR SMALL CROSS FLOW

TRANSFORMATION TO SIMILARITY VARIABLES

The methods of local similarity (refs. 7, 8, and 9, for example) provide convenient and accurate procedures for computing heat transfer, skin friction, and other laminar boundary-layer characteristics. In the present analysis the method of reference 9 will be adopted with emphasis placed on computing the distribution of heating. The absolute level of heating can be established from the results of reference 10 where a solution for the three-dimensional stagnation point is presented.

The boundary-layer equations for small cross flow (eqs. (13), (14), (16), and (18)) are first transformed to similarity variables ξ and η (see ref. 9) which are defined here as

$$\left.\begin{aligned}\xi&=\int_{s_o}^{s}\rho_w\mu_wu_ee_2^2ds\\ \eta&=\frac{u_ee_2}{\sqrt{2(\xi-\bar{\xi})}}\int_0^z\rho dz\end{aligned}\right\} \quad (19)$$

where $s=s_o$ at $x=x_o$. The quantity $\bar{\xi}$ is a function of ξ as determined in reference 9. It is understood that ξ is measured separately along each streamline for which the quantities ρ_w, μ_w, u_e, and e_2 are specified functions of s. Generally, ξ would be a different function for each streamline.

In order to satisfy continuity (eq. (13)), a stream function $\psi(s,z)$ is defined as

$$\left.\begin{aligned}\frac{\partial\psi}{\partial z}&=\rho ue_2\\ \frac{\partial\psi}{\partial s}&=-\rho we_2\end{aligned}\right\} \quad (20)$$

A related function $f(\xi,\eta)$ is also introduced as

$$f=\frac{1}{\sqrt{2(\xi-\bar{\xi})}}\psi \quad (21)$$

so that from equations (19)

$$\frac{\partial f}{\partial\eta}=\frac{u}{u_e} \quad (22)$$

Since

$$t_e\left[\left(\frac{\partial f}{\partial\eta}\right)^2-\frac{\rho_e}{\rho}\right]=\left(\frac{\partial f}{\partial\eta}\right)^2-\zeta+t_e\left(\frac{t}{t_e}-\frac{\rho_e}{\rho}\right)$$

equations (14), (16), and (18) become

$$2(\xi-\bar{\xi})\left(\frac{\partial f}{\partial\eta}\frac{\partial^2f}{\partial\xi\partial\eta}-\frac{\partial^2f}{\partial\eta^2}\frac{\partial f}{\partial\xi}\right)-\left(1-\frac{d\bar{\xi}}{d\xi}\right)f\frac{\partial^2f}{\partial\eta^2}=-\frac{2(\xi-\bar{\xi})}{u_et_e}\frac{du_e}{d\xi}\left[\left(\frac{\partial f}{\partial\eta}\right)^2-\zeta+t_e\left(\frac{t}{t_e}-\frac{\rho_e}{\rho}\right)\right]+\frac{\partial}{\partial\eta}\left(\varphi\frac{\partial^2f}{\partial\eta^2}\right) \quad (23)$$

$$2(\xi-\bar{\xi})\left(\frac{\partial f}{\partial\eta}\frac{\partial\zeta}{\partial\xi}-\frac{\partial\zeta}{\partial\eta}\frac{\partial f}{\partial\xi}\right)-\left(1-\frac{d\bar{\xi}}{d\xi}\right)f\frac{\partial\zeta}{\partial\eta}=\frac{\partial}{\partial\eta}\left\{\varphi\left[\frac{\partial\zeta}{\partial\eta}+\frac{1-N_{Pr}+F}{N_{Pr}}\frac{\partial t}{\partial\eta}\right]\right\} \quad (24)$$

$$2(\xi-\bar{\xi})\left[\frac{\partial f}{\partial\eta}\frac{\partial}{\partial\xi}(e_2v)-\frac{\partial}{\partial\eta}(e_2v)\frac{\partial f}{\partial\xi}\right]-\left(1-\frac{d\bar{\xi}}{d\xi}\right)f\frac{\partial}{\partial\eta}(e_2v)=\frac{2(\xi-\bar{\xi})}{\rho_w\mu_wt_ee_2}K\left[\left(\frac{\partial f}{\partial\eta}\right)^2-\zeta+t_e\left(\frac{t}{t_e}-\frac{\rho_e}{\rho}\right)\right]+\frac{\partial}{\partial\eta}\left[\varphi\frac{\partial}{\partial\eta}(e_2v)\right] \quad (25)$$

where

$$\zeta=\frac{H}{H_e}\text{ and }t=\frac{h}{H_e}=\zeta-(1-t_e)\left(\frac{\partial f}{\partial\eta}\right)^2$$

A new dependent variable V involving the cross-flow velocity v is now introduced into equation (25). This variable is defined by the relation

$$V=\frac{e_2v}{G} \quad (26)$$

where

$$G=\frac{2(\xi-\bar{\xi})}{\rho_w\mu_wt_ee_2}K \quad (27)$$

For a given streamline, G is considered a function of ξ only since all quantities in equation (27) are

presumed known along each streamline. Also, V is considered a function of ξ and η on a given streamline although it is a different function for each streamline. Equation (25) then becomes

$$2(\xi-\bar{\xi})\left(\frac{\partial f}{\partial \eta}\frac{\partial V}{\partial \xi}-\frac{\partial f}{\partial \xi}\frac{\partial V}{\partial \eta}\right)-\left(1-\frac{d\bar{\xi}}{d\xi}\right)f\frac{\partial V}{\partial \eta}+\frac{2(\xi-\bar{\xi})}{G}\frac{dG}{d\xi}\frac{\partial f}{\partial \eta}V=\left(\frac{\partial f}{\partial \eta}\right)^2-\zeta+t_e\left(\frac{t}{t_e}-\frac{\rho_e}{\rho}\right)+\frac{\partial}{\partial \eta}\left(\varphi\frac{\partial V}{\partial \eta}\right) \quad (28)$$

LOCAL SIMILARITY

In accordance with the usual procedure for similar solutions, the ξ derivatives of the profile functions f, ζ, and V are assumed negligible compared to the other terms in equations (23), (24), and (28). The first term on the left-hand side of each of these three equations then drops out. It is then possible to show by means of a transformation of coordinates and profiles of the form

$$\eta_1=\left(1-\frac{d\bar{\xi}}{d\xi}\right)^{1/2}\eta$$

$$\frac{\partial f_1}{\partial \eta_1}=\frac{\partial f}{\partial \eta}$$

$$\zeta_1=\zeta$$

$$\frac{v_1}{u_e}=\frac{v}{u_e}$$

that the value of $d\bar{\xi}/d\xi$ is arbitrary for similar flows and hence may be taken as zero.

In order to further simplify the problem of solving equations (23), (24), and (28), the following assumptions are made:

$$\left.\begin{aligned}&\varphi=N_{Pr}=1\\&\frac{t}{t_e}=\frac{\rho_e}{\rho}\\&F=0\\&t_w=\text{Constant}\end{aligned}\right\} \quad (29)$$

Reference 9 shows that, if the assumptions regarding the gas properties are confined to the solution of the differential equations, the effect on the distribution of heating (as opposed to the absolute value of heating) is generally small for two-dimensional or axisymmetric bodies. The same result must apply to the arbitrary three-dimensional body if the cross flow is small. The assumption of an isothermal wall (that is, $dt_w/ds=0$) has a negligible effect on the distribution of the heat-transfer coefficient except when $t_w \to t_{aw}$.

Assuming local similarity and introducing the conditions of equations (29) results in the final differential equations which are

Streamwise momentum:

$$f'''+ff''=\beta[f'^2-(1-t_w)\theta-t_w] \quad (30)$$

Energy:

$$\theta''+f\theta'=0 \quad (31)$$

Cross-flow momentum:

$$V''+fV'-\beta^* f'V=(1-t_w)\theta+t_w-f'^2 \quad (32)$$

where

$$\theta=\frac{\zeta-t_w}{1-t_w} \quad (33)$$

$$\beta=\frac{2(\xi-\bar{\xi})}{u_e t_e}\frac{du_e}{d\xi} \quad (34)$$

$$\beta^*=\frac{2(\xi-\bar{\xi})}{G}\frac{dG}{d\xi} \quad (35)$$

The prime denotes total differentiation with respect to η which is now possible because of the assumption of local similarity. That is, even though β and β^* are considered functions of ξ, equations (30) to (32) are treated as total differential equations with β and β^* as parameters. The boundary conditions for equations (30) to (32) are

$$\left.\begin{aligned}&f(0)=0\\&f'(0)=V(0)=\theta(0)=0\\&f'(\infty)=\theta(\infty)=1\\&V(\infty)=0\end{aligned}\right\} \quad (36)$$

SOLUTIONS TO SIMILAR EQUATIONS

EXACT SOLUTIONS

Solutions to equations (30) and (31) which are

the similar boundary-layer equations for two-dimensional or axisymmetric flow are available in references 9, 11, and 14. With f and θ known from these solutions, equation (32) is linear in V; however, no general solution was found. Consequently, the problem was programed for numerical solution on the IBM type 7090 electronic data processing machine. A step size of $\Delta\eta=0.1$ was used in these solutions; otherwise, the procedure and accuracy were similar to that described in reference 11.

About 35 solutions were obtained and the resulting values of $-V'_w$ are given in table I. For convenience the corresponding values of f''_w and θ'_w are also tabulated. Typical profiles of V are shown in figures 1 to 3. The solid lines are from exact solutions of equation (32), and the dashed lines are from an approximate solution which is presented in the appendix and discussed in the next section. Note that V is negative for all values of β and β^* used. Also, $-V$ decreases as t_w decreases indicating that the cross-flow velocity is reduced as the ratio of wall enthalpy to total enthalpy is reduced. This trend would be expected according to the previous discussion of equation (12). The cross-flow parameter $-V$ also decreases as β and β^* increase. The resulting effect on the cross-flow velocity profile v/u_e cannot be determined without also specifying the value of G and e_2 as indicated by equation (26). These various parameters may be expressed in terms of convenient physical quantities as is discussed in the section entitled "Criteria for Small Cross Flow."

Closed-form solutions to equation (32) are possible for $\beta^*=0$ and -1. For $\beta^*=0$ the general solution is

$$V=\frac{1}{\beta}(\theta-f') \qquad (\beta^*=0) \tag{37}$$

and for $\beta^*=-1$ the solution is

$$V=V'_w\theta'\int_0^\eta \frac{d\eta}{\theta'}+\theta'\int_0^\eta \frac{1}{\theta'}\left[\int_0^\eta (\zeta-f'^2)d\eta\right]d\eta \qquad (\beta^*=-1) \tag{38}$$

The corresponding wall derivatives are

$$V'_w=\frac{1}{\beta}(\theta'_w-f''_w) \qquad (\beta^*=0) \tag{39}$$

$$V'_w=-\int_0^\infty (\zeta-f'^2)d\eta \qquad (\beta^*=-1) \tag{40a}$$

By use of equation (30), integration by parts, and the introduction of the definition of θ^*_{tr}, equation (40a) may be written as

$$V'_w=\frac{1}{\beta}(\theta^*_{tr}-f''_w) \qquad (\beta^*=-1) \tag{40b}$$

Values of θ^*_{tr} are tabulated in references 9, 11 (values for $\lambda=1$ must be used here), and 14. Also note that at $\beta=0$, $\theta=f'$, and equation (40a) may be integrated to yield

$$V'_w=-f''_w-\lim_{\eta\to\infty}(\eta-f)t_w=-0.4696-1.2168t_w \qquad (\beta^*=-1;\ \beta=0)$$

APPROXIMATE SOLUTION

For convenience in interpolation an approximate solution to equation (32) was also obtained. Details of this solution are given in the appendix. The value of V'_w is computed from the simultaneous equations

$$V'_w=\frac{V'_{w,\beta^*=-1}}{1+\frac{1+\beta^*}{60}f''_w\eta_e^3} \tag{41}$$

$$V'_w=-\frac{1}{5}t_w\eta_e-\frac{1-t_w}{60}\theta'_w\eta_e^2 \tag{42}$$

where η_e is the value of η at which the exterior boundary condition $V=0$ was applied. The quantity $V'_{w,\beta^*=-1}$ is taken from equation (40). Values of $-V'_w$ from equations (41) and (42) are plotted against positive values of β in figure 4(a) for various values of β^* and t_w. Also shown in this figure (the isolated points—circles, squares, and diamonds) are the results of the exact solutions from table I. For $\beta^*=0$ and -1, calculated values from equations (39) and (40) are shown as solid lines. Over the range of conditions shown, the approximate solution is satisfactory.

The variation of V'_w with negative values of β and $\beta^*=0$ is shown in figure 4(b). This figure shows that $-V'_w$ increases rapidly for increasing negative values of β but remains finite up to the separation point of the streamwise flow ($f''_w=0$).

TABLE I.—PARAMETERS FROM SIMILAR SOLUTIONS

[Perfect gas with $N_{Pr}=\varphi=1$]

t_w	β	f''_w	θ'_w	$-V'_w$ for β^* of									
				−1	0	3	4	6	8	10	12	14	20
0	−0.3264	0	0.2478	1.8588	0.7591								
0	−.3884	.1400	.3527	1.2873	.5476								
0	0	.4696	.4696	.4696									
0	.2	.5233	.4821	.3881	.2060	0.1143	0.1027						
0	.5	.5811	.4942	.3146	.1738		.0901	0.0770					
0	1.0	.6489	.5067	.2456	.1422				0.0593	0.0540			
0	1.5	.6987	.5147	.2049	1226					.0489	0.0453		
0	2.0	.7386	.5206	.1775	.1090						.0419	0.0393	
0	2.6	.7783	.5260	.1542	.0970							.0364	0.0313
0	3.2	.8119	.5302	.1372	.0880							.0342	.0295
0	3.8	.8412	.5336	.1242	.0809								.0280
0	4.4	.8672	.5364	.1137	.0752								
.5	−.2623	0	.3076	2.3130	1.1727								
.5	−.2	.2507	.4152	1.4825	.8225								
.5	0	.4696	.4696	1.0780									
.5	.2	.6070	.4951	.8995	.5592	.3721							
.5	.5	.7609	.5185	.7468	.4849		.3104						
.5	1.0	.9548	.5421	.6056	.4127				.2317				
.5	1.5	1.1090	.5574	.5221	.3678					.2021			
.5	2.0	1.2405	.5686	.4652	.3360								
.5	2.6	1.3788	.5788	.4162	.3077							.1648	
.5	3.2	1.5021	.5869	.3798	.2860								
.5	3.8	1.6143	.5936	.3514	.2686								
1.0	−.1988	0	.3258	2.9447	1.6388								
1.0	−.16	.1905	.4023	2.2594	1.3237								
1.0	0	.4696	.4696	1.6864									
1.0	.2	.6867	.5069	1.3925	.8993	.6183							
1.0	.5	.9277	.5390	1.1548	.7774		.5142						
1.0	1.0	1.2326	.5705	.9402	.6621				.3859				
1.0	1.5	1.4772	.5906	.8140	.5910					.3367			
1.0	2.0	1.6872	.6052	.7282	.5410						.3027		
1.0	2.6	1.9092	.6185	.6538	.4964								
1.0	3.2	2.1081	.6290		.4622								
1.0	3.6	2.2308	.6349	.5690	.4433								

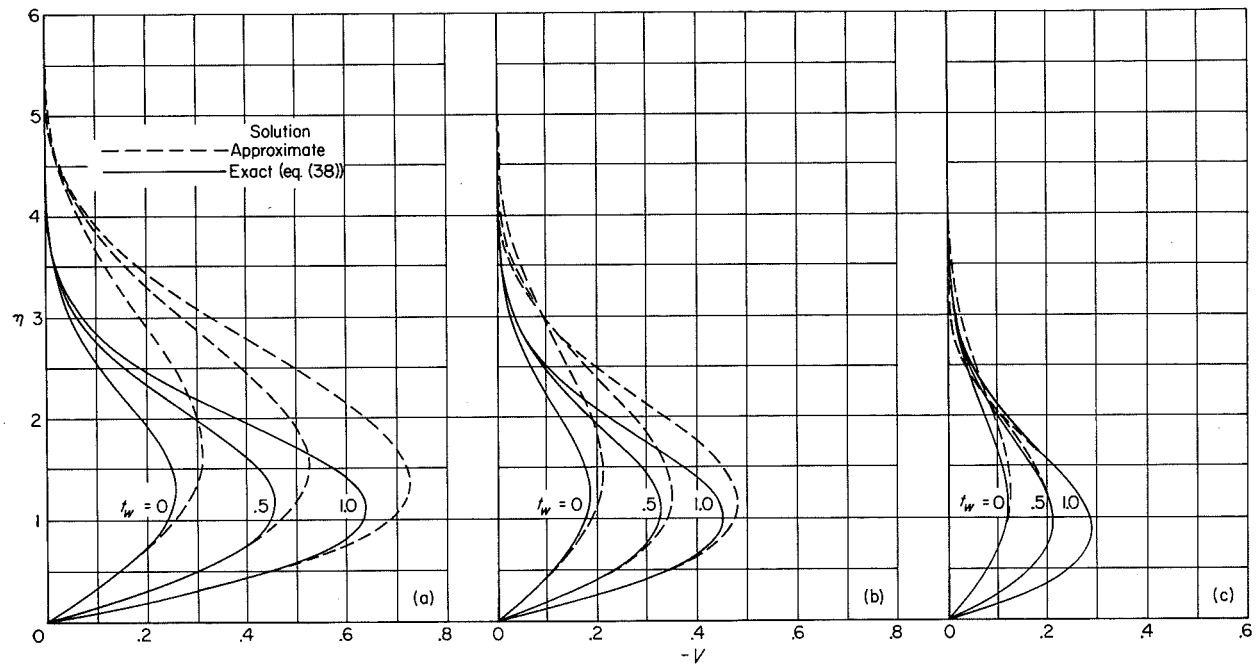

(a) $\beta=0.5$. (b) $\beta=1.0$. (c) $\beta=2.0$.

FIGURE 1.—Typical profiles for cross-flow velocity parameter V. Perfect gas with $N_{Pr}=\varphi=1$. $\beta^*=-1$.

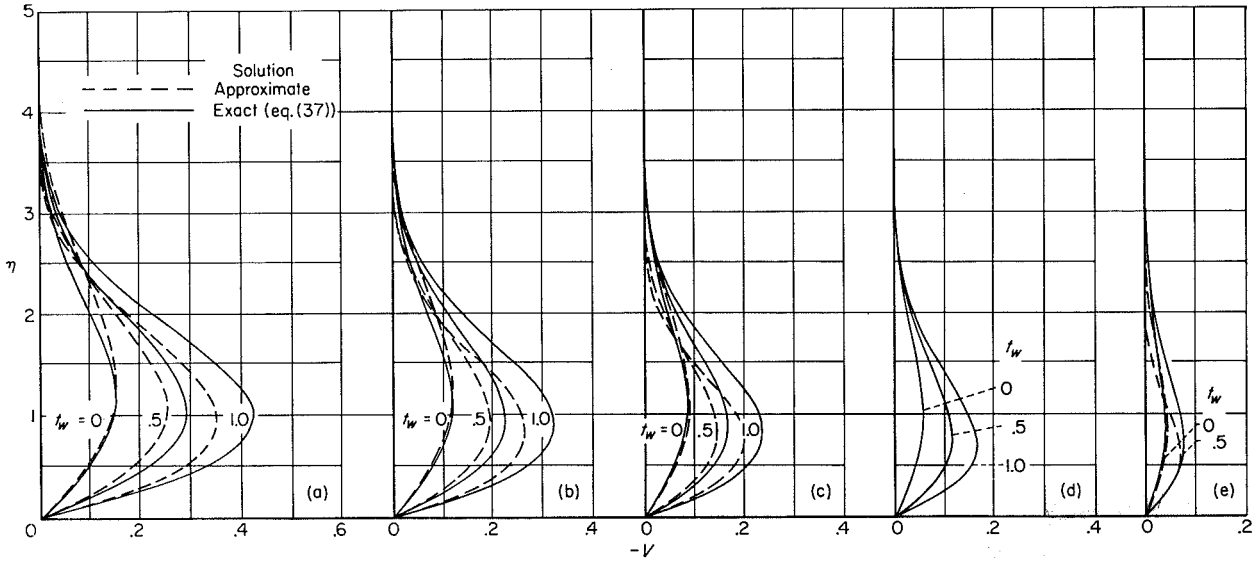

(a) $\beta=0.2$. (b) $\beta=0.5$. (c) $\beta=1.0$. (d) $\beta=2.0$. (e) $\beta=3.8$.

FIGURE 2.—Typical profiles for V. $\beta^*=0$.

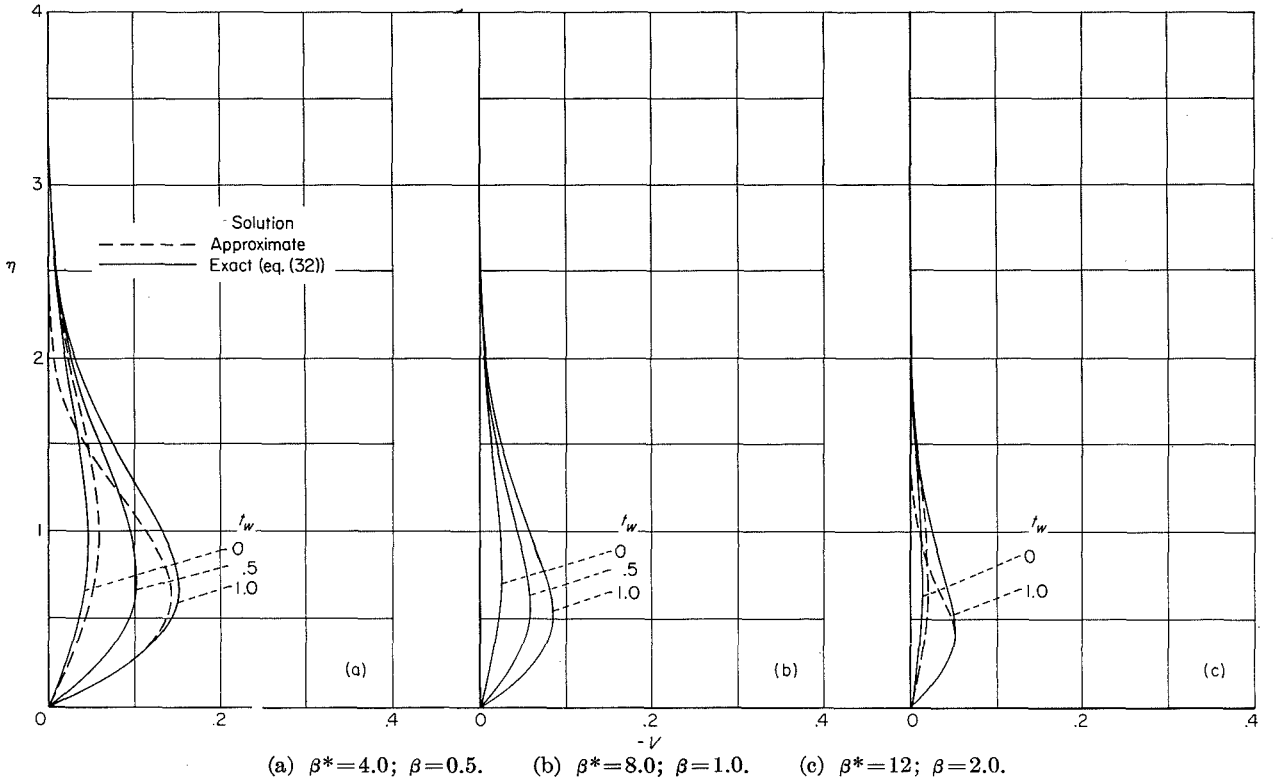

(a) $\beta^*=4.0$; $\beta=0.5$. (b) $\beta^*=8.0$; $\beta=1.0$. (c) $\beta^*=12$; $\beta=2.0$.

FIGURE 3.—Typical profiles for V. $\beta^* \geqq 4.0$.

The cross-flow profiles $V(\eta)$ may also be computed from the approximate solution as indicated in the appendix. Typical results are shown in figures 1 to 3 as the dashed lines. The approximate profiles are in good agreement with the exact profiles in the region near the wall but the agreement is not so good near the outer portion of the boundary layer particularly for $\beta^*=-1$ and small values of β. However, the main purpose of the approximate solution in the present analysis is to provide values of V_w' which from figure 4 appear to be sufficiently accurate.

SOLUTIONS FOR $\beta \to \infty$

For application to flows where β is large the behavior of V for $\beta \to \infty$ is useful. From equations (30) and (32) it is evident that $V \to 0$ as $\beta \to \infty$ which indicates that the cross flow tends to decrease as β increases.

In appendix B of reference 9 it was shown that for $\beta \to \infty$ the wall shear parameter, which for the present application is the streamwise shear parameter, is given by the expression

$$f_w''=\frac{2}{3}\sqrt{3\beta}t_w^{3/4} \qquad (\beta \to \infty) \tag{43}$$

and that the heat-transfer parameter θ_w' approaches finite values (tabulated in ref. 9) which, for zero yaw, depend only on t_w. From these results and equation (39) the expression for V_w' for $\beta \to \infty$ and $\beta^*=0$ is

$$V_w'=\frac{\theta_{w,\beta\to\infty}'}{\beta}-\frac{2}{3}\sqrt{\frac{3}{\beta}}\,t_w^{3/4} \qquad (\beta^*=0;\beta\to\infty) \tag{44}$$

For $\beta^*=-1$ the limiting expression for V_w' from equations (40b) and (43) is

$$V_w'=\frac{1}{\beta}\theta_{tr,\beta\to\infty}^*-\frac{2}{3}\sqrt{\frac{3}{\beta}}\,t_w^{3/4} \qquad (\beta^*=-1;\beta\to\infty) \tag{45}$$

Values of θ_w' and θ_{tr}^* for $\beta \to \infty$ are given in the following table (from ref. 9 for $\lambda=1$):

t_w	θ_w'	θ_{tr}^*
0	0.5894	0.3549
.5	.7230	.1965
1.0	.7979	0

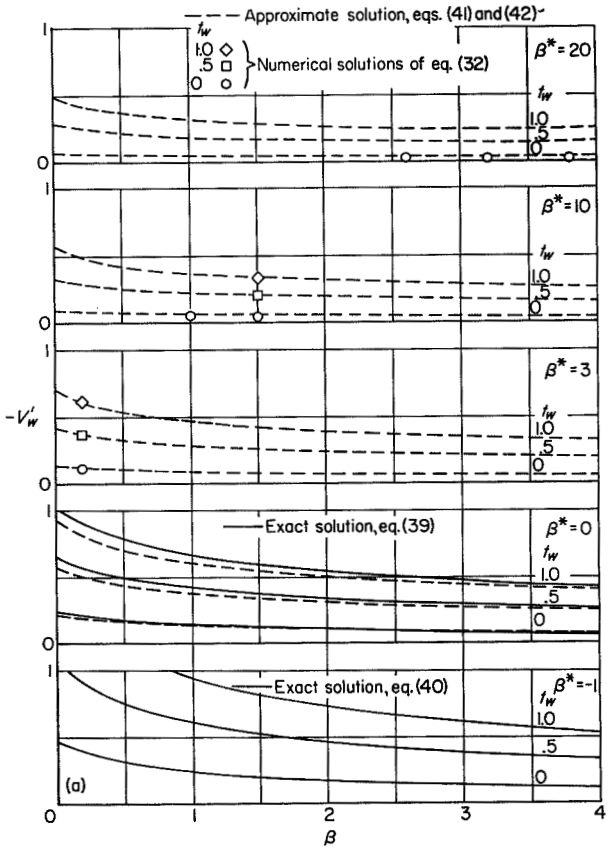

(a) $\beta>0$.

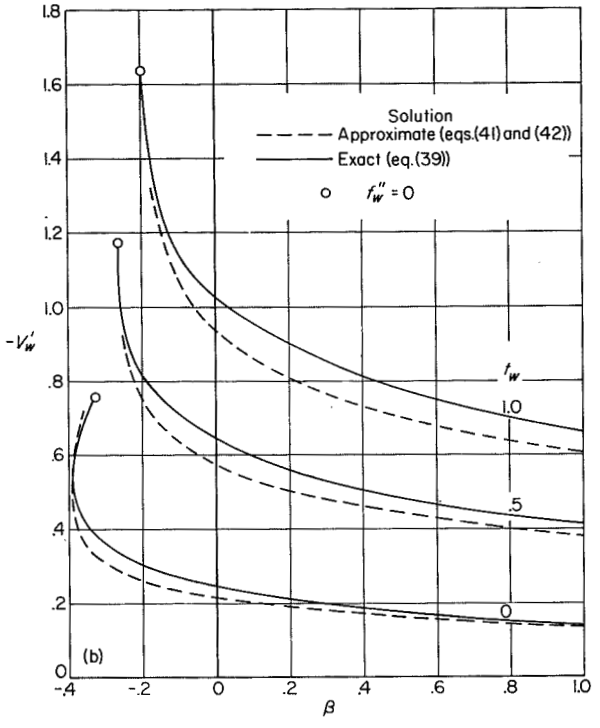

(b) $\beta<1.0$; $\beta^*=0$.

FIGURE 4.—Variation of cross-flow skin-friction parameter V'_w with β for several values of β^* and t_w. Perfect gas with $N_{Pr}=\varphi=1$.

FIGURE 4.—Concluded.

CRITERIA FOR SMALL CROSS FLOW

Approximate solutions to many nonlinear problems can be obtained by the use of simplifying assumptions that reduce the equations to linear form for some particular range of conditions. The results of the linearized solutions can then be used to determine the range of conditions for which the assumptions are valid.

The present situation is analogous in that the solutions to the linearized cross-flow momentum equation, as well as other physical conditions of the problem, are used to determine the maximum values that a physical quantity may have for the assumption of small cross flow to be valid. This physical quantity is the ratio of local cross-flow velocity to streamwise velocity v/u which, for small cross flow, must satisfy the inequality

$$\left(\frac{v}{u}\right)^2 \ll 1 \tag{46}$$

In order to evaluate the ratio v/u a general expression for G is first obtained by elimination of $(\xi-\bar{\xi})$ between equations (34) and (27), use of equations (10), (11), and (19), and the definitions of K, s, and n. The result is

$$G=-\beta u_e e_2 \frac{\partial p/\partial n}{\partial p/\partial s} \tag{47}$$

From the definition of V (eq. (26)) the cross-flow velocity profile may then be written as

$$\frac{v}{u_e}=-\beta\frac{\partial p/\partial n}{\partial p/\partial s}V \tag{48}$$

The value of v/u then follows from equation (22) and is

$$\frac{v}{u}=-\beta\frac{\partial p/\partial n}{\partial p/\partial s}\frac{V}{f'}$$

From the boundary conditions given in equations (36) it can be shown that the ratio v/u has its maximum value at $\eta=0$; that is,

$$\left(\frac{v}{u}\right)_{max}=-\beta\frac{\partial p/\partial n}{\partial p/\partial s}\frac{V'_w}{f''_w} \tag{49}$$

The quantity $-\beta \frac{V'_w}{f''_w}$ is plotted in figure 5 as a function of β for $t_w=0$, 0.5, and 1.0 and for values of β^* from -1 to 20. The values of V'_w used in this figure were obtained from the approximate equations (41) and (42) except where noted. Isolated points from the exact numerical solutions for V'_w are also shown. All values of f''_w were taken from numerical solutions to equations (30) and (31).

Thus, in order to apply the criteria of inequality (46) to any given body shape the values of β, β^*, t_w, and $\frac{\partial p/\partial n}{\partial p/\partial s}$ are required along each streamline. Then with the aid of figure 5 equation (49) can be evaluated.

A convenient expression for β^* in terms of physical quantities can be obtained by first combining equations (34) and (35) to give

$$\beta^*=\beta t_e \frac{\frac{1}{G}\frac{dG}{ds}}{\frac{1}{u_e}\frac{du_e}{ds}} \tag{50}$$

Then, with the use of equation (47) for G and equation (10) for $\partial p/\partial s$, equation (50) can be written as

$$\beta^*=\frac{t_e \rho_e u_e}{\frac{\partial p}{\partial n}\Delta n}\frac{d}{ds}\left[\beta u_e \Delta n \frac{\partial p/\partial n}{-(\partial p/\partial s)}\right] \tag{51}$$

The parameter β is independent of the cross flow and hence may be computed by the method of reference 9. Application of the simple local similarity method of reference 9 to the present problem and the use of the simplifying assumptions of equations (29) result in the equation

$$\beta=\frac{2\frac{du_e}{ds}}{\frac{p_e}{p_o}u_e^2 t_e(\Delta n)^2}\left\{\int_{s_o}^{s}\frac{p_e}{p_o}u_e(\Delta n)^2 ds+\left[\frac{u_e^2 t_e \beta(\Delta n)^2}{2\frac{du_e}{ds}}\right]\right\} \tag{52}$$

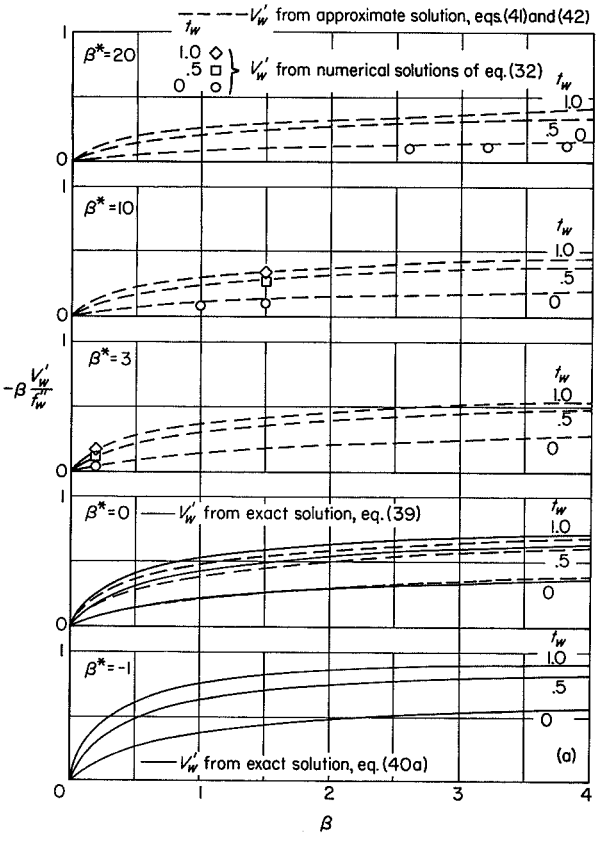

(a) $\beta>0$.

FIGURE 5.—Variation of small-cross-flow parameter $-\beta \frac{V'_w}{f''_w}$ with β for several values of β^* and t_w. Perfect gas with $N_{Pr}=\varphi=1$.

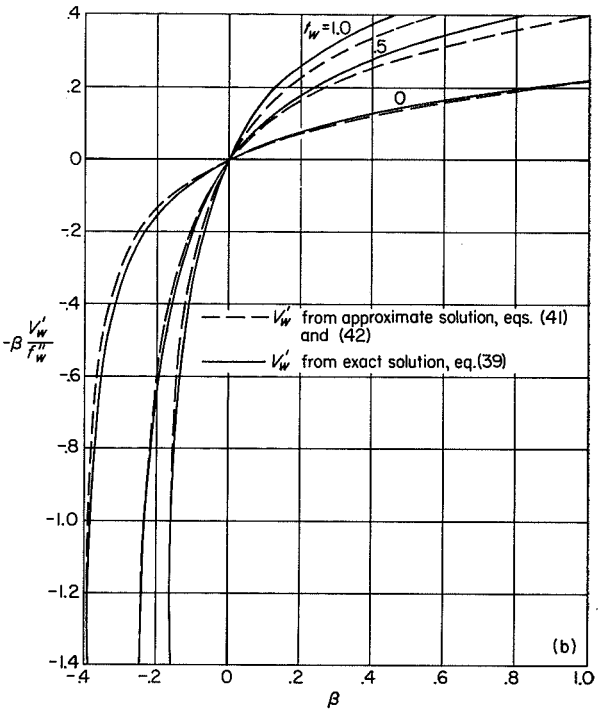

(b) $\beta<1.0$; $\beta^*=0$.

FIGURE 5.—Concluded.

In both equations (51) and (52) the metric coefficient e_2 has been approximated from equations (1) as

$$e_2 \approx \frac{\Delta n}{\Delta y} \tag{53}$$

where Δn is the normal spacing between adjacent streamlines. Then, since Δy is constant along a given streamline, it cancels out of equations (51) and (52).

The value of β at $s=s_o$ as required in the last term of equation (52) may be evaluated approximately for a blunt-nosed body from the results of reference 10. If $s=s_o$ is in the vicinity of the stagnation point, then the value of β_o may be assumed the same as that at the stagnation point. From reference 10 it can be seen that $\theta'_{w,sp}$ is approximately a linear function of the principal velocity gradient ratio which may be expressed as

$$\left[\frac{(du_e/ds)_{min}}{(du_e/ds)_{max}}\right]_{sp} = \frac{R^*_{min}}{R^*_{max}} \tag{54}$$

for a Newtonian pressure distribution. Then from the results of reference 11, for example, it may also be assumed that $\theta'_{w,sp}$ varies linearly with β_{sp} between the limits of $\beta_{sp}=0.5$ for the axisymmetric body and $\beta_{sp}=1.0$ for the two-dimensional (unyawed) body. Consequently, when these results are used with the assumption of small cross flow, the expression for β_o is

$$\beta_o \approx \beta_{sp} \approx 1 - \frac{1}{2}\frac{R^*_{min}}{R^*_{max}} \tag{55}$$

The value of β^* at $s=0$ is obtained from equation (50) evaluated at the limit as $s \to 0$. The result is

$$\beta^*_{sp} = 2\beta_{sp} \tag{56}$$

since as $s \to 0$, e_2, $\partial p/\partial n$, $\partial p/\partial s$, and u_e all approach zero but du_e/ds remains finite. Equations (55) and (56) show that $\beta^*_{sp} \geqq 1$ and equation (51) indicates that if $\partial p/\partial s$ is negative, as it would be over the entire forward portion of a blunt body, β^* would remain positive until the quantity

$$\beta u_e \Delta n \frac{|\partial p/\partial n|}{-(\partial p/\partial s)}$$

attains its maximum.

Evaluating the cross flow on any particular body obviously requires a detailed analysis; however, a few remarks can now be made to indicate general trends. Figure 5(a) and equation (49) show that for $\beta^* > 0$ and $0 < \beta < 4$, inequality (46), which establishes the criteria for small cross flow, would be satisfied if the pressure-gradient parameter $\left|\frac{\partial p/\partial n}{\partial p/\partial s}\right| < 1$ and $t_w \approx 0$. For values of the enthalpy ratio in the range of $0.5 < t_w < 1$, such as might apply to wind-tunnel tests, the pressure-gradient parameter would have to be less than about 0.5 to have small cross flow. When β^* is negative, the parameter $-\beta\frac{V'_w}{f''_w}$ increases so that the pressure-gradient parameter must be correspondingly smaller if $(v/u)^2$ is to remain small. For negative values of β such as those that occur when the streamwise flow approaches separation, figure 5(b) indicates that the cross flow would probably become very large and the assumption of small cross flow would be invalid.

Equations (41) and (43) to (45) show that as $\beta \to \infty$ the parameter $\beta\frac{V'_w}{f''_w} \to -1$ independent of t_w and β^*. Hence, for very large values of β the cross flow would be small if $\left(\frac{\partial p/\partial n}{\partial p/\partial s}\right)^2 \ll 1$.

Note from equation (48) that v always has the opposite sign from $\partial p/\partial n$ since V is always negative (at least for all values of β^* considered), and the quantity $\frac{\beta}{\partial p/\partial s}$ is also always negative from equations (52) and (10). Thus, as would be expected for a similar flow, the direction of v is determined solely by the local direction of the cross-flow pressure gradient. Consequently, in flows where this pressure gradient is changing rapidly in magnitude or direction, the cross-flow velocity profiles could not be similar because of the "viscous lag" of the boundary layer. This phenomenon is discussed in detail in reference 3.

EQUATIONS FOR HEAT TRANSFER AND SKIN FRICTION

When the cross flow is small, that is, when inequality (46) is satisfied, the heat transfer and streamwise skin friction are independent of the cross flow, as indicated by equations (13), (14), and (16). With a simple modification, the results of reference 9 then apply directly to the arbitrary three-dimensional body. The distribution of the

heat-transfer coefficient along a streamline is given by the relation (ref. 9)

$$\frac{q_w}{q_{w,o}}\frac{(t_{aw}-t_w)_o}{t_{aw}-t_w}=\left[\frac{p_e}{p_o}\frac{t_o}{t_e}\frac{\beta_o}{\beta}\frac{du_e/ds}{(du_e/ds)_o}\right]^{1/2}\frac{1+P\beta^N}{Q+R\beta^N}\left(\frac{Q+R\beta^N}{1+R\beta^N}\right)_o \quad (57)$$

which applies for $\beta>0$ and an isothermal wall. The quantities P, Q, R, and N are functions of t_w and t_s as tabulated and plotted in reference 9. For the present application $t_s=1$. The heat-transfer distribution $q_w/q_{w,o}$ may be computed from equation (57) by use of the expression for t_{aw} from reference 9

$$\left.\begin{aligned} t_{aw}&=t_e+\sqrt{N_{Pr}}\,(1-t_e)\\ t_e&=1-\frac{u_e^2}{2H_e}\end{aligned}\right\} \quad (58)$$

The parameter β is a function of s as given by equation (52), and β_o is given by equation (55) for a blunt body.

Substituting equation (52) into equation (57) shows that the present expression for the heat-transfer ratio is similar to the corresponding expression that would be obtained from reference 6 except for the factors $\frac{t_{aw}-t_w}{(t_{aw}-t_w)_o}$, $\frac{1+P\beta^N}{Q+R\beta^N}$, and $\left(\frac{Q+R\beta^N}{1+R\beta^N}\right)_o$ which have no counterpart in reference 6 because of the assumptions of a highly cooled wall and a flat-plate enthalpy profile. The effect of these factors for many practical applications would not exceed about 20 percent as shown in reference 9.

The correct limiting form of $q_{w,o}$ cannot be obtained from reference 6 without an accurate evaluation of e_2 (h_2 in the notation of ref. 6) in the stagnation region. The correct limiting form is accounted for in the present analysis by an evaluation of β_o (from eq. (55) for a blunt body). If the proper value of β_o is used in equation (57) then Δn can probably be assumed constant in equation (52) since sample calculations on two-dimensional cylinders (normal to the stream velocity) and equivalent bodies of revolution indicate that Δn has little effect on the heat-transfer ratio.

The streamwise skin friction is obtained from reference 9 as

$$\tau_x=u_e\left(\frac{\rho_w\mu_w}{\beta t_e}\frac{du_e}{ds}\right)^{1/2}f_w'' \quad (59)$$

The cross-flow skin friction

$$\tau_y=\mu_w\left(\frac{\partial v}{\partial z}\right)_w$$

is from equations (19), (34), and (48)

$$\tau_y=-u_e\left(\frac{\rho_w\mu_w}{\beta t_e}\frac{du_e}{ds}\right)^{1/2}\beta\frac{\partial p/\partial n}{\partial p/\partial s}V_w' \quad (60)$$

Hence, the ratio of cross-flow skin friction to streamwise skin friction is

$$\frac{\tau_y}{\tau_x}=-\beta\frac{\partial p/\partial n}{\partial p/\partial s}\frac{V_w'}{f_w''} \quad (61)$$

A comparison of equation (61) with equation (49) shows that for small cross flow

$$\left(\frac{\tau_y}{\tau_x}\right)^2\ll 1.0$$

as would be expected. It then follows that the total component of skin friction is

$$\tau\approx\tau_x$$

APPLICATION OF SMALL-CROSS-FLOW THEORY TO YAWED INFINITE CYLINDER

The boundary layer on the yawed infinite cylinder exhibits one of the principal characteristics of three-dimensional boundary layers, namely, cross-flow velocities which generally would not be small. Since similar solutions of the complete boundary-layer equations are already available for the yawed cylinder (refs. 9, 11, and 15, for example), this configuration is used for comparison with the results of the small-cross-flow theory.

VELOCITY PROFILES AND SKIN FRICTION

The streamwise and cross-flow velocities u and v in the coordinate system s,n are written in terms of the Cartesian coordinate system $\bar{x},\bar{y}$ and corresponding velocities $\bar{u}$ and $\bar{v}$ as applied to the yawed infinite cylinder (ref. 11). Thus, barred quantities refer to results obtained from the exact solutions of reference 11 and unbarred quantities are from the small-cross-flow theory.

The expressions for v and u can then be derived from the geometry of the problem as illustrated in figure 6(a) and from the definitions $\bar{f}'=\bar{u}/\bar{u}_e$ and $\bar{g}=\bar{v}/\bar{v}_e$; thus,

$$\frac{v}{u_e}=-(\bar{f}'-\bar{g})\cos^2\alpha_e\tan\alpha_e \tag{62}$$

(The negative sign is used in eq. (62) so that the direction of v will be consistent with the s,n coordinate system as indicated in figure 6(a). Thus, when $\bar{\beta}$ is positive, $\bar{f}'>\bar{g}$, and when $\bar{\beta}$ is negative, $\bar{f}'<\bar{g}$, as indicated by the wall derivatives of these quantities tabulated in ref. 9.)

$$\frac{u}{u_e}=\bar{f}'\sin^2\alpha_e+\bar{g}\cos^2\alpha_e \tag{63}$$

where

$$\tan\alpha_e=\frac{\bar{u}_e}{\bar{v}_e}$$

$$\tan\alpha=\frac{\bar{u}_e}{\bar{v}_e}\frac{\bar{f}'}{\bar{g}}$$

Hence, from the adiabatic energy equation

$$H_e=h_e+\frac{\bar{u}_e^2}{2}+\frac{\bar{v}_e^2}{2}=h_e+\frac{u_e^2}{2}$$

and from the definitions of t_e and λ (the reciprocal of the corresponding yaw parameter t_s in ref. 9)

$$\frac{v}{u_e}=-\frac{\lambda-1}{\lambda(1-t_e)}\sqrt{\frac{1-\lambda t_e}{\lambda-1}}(\bar{f}'-\bar{g}) \tag{64}$$

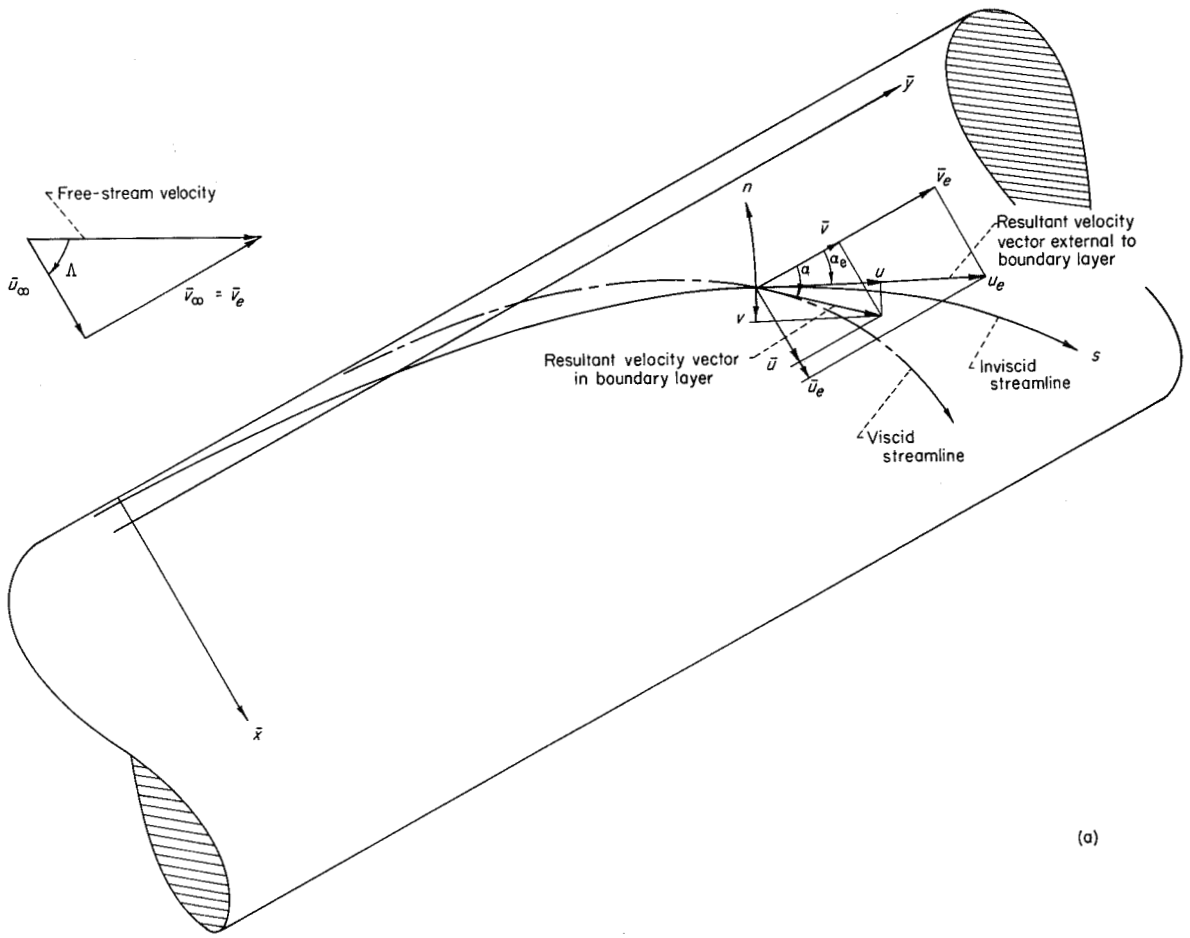

(a) Velocity components.

FIGURE 6.—Definition sketch of various flow components on yawed infinite cylinder.

$$\frac{u}{u_e}=\frac{\lambda-1}{\lambda(1-t_e)}\bar{g}+\frac{1-\lambda t_e}{\lambda(1-t_e)}\bar{f}' \tag{65}$$

where $\bar{f}'$ and $\bar{g}$ are functions of $\bar{\beta}$ and $\bar{\eta}$ from the solutions for the yawed infinite cylinder. The profiles given by equations (64) and (65) are to be compared to the corresponding profiles from the small-cross-flow theory. From equations (48) and (22) these profiles are

$$\frac{v}{u_e}=-\beta\frac{\partial p/\partial n}{\partial p/\partial s}V \tag{66}$$

$$\frac{u}{u_e}=f' \tag{67}$$

where f' and V are functions of β, β^*, and η. Thus, before comparisons can be made, it is necessary to derive equations relating the parameters β and β^* to $\bar{\beta}$ as well as the independent variables η and $\bar{\eta}$ as applied to the yawed infinite cylinder.

On the yawed infinite cylinder (fig. 6)

$$\Delta n=\sin\alpha_e\Delta\bar{y}=\frac{\bar{u}_e}{u_e}\Delta\bar{y} \tag{68}$$

where

$$\Delta\bar{y}=\text{Constant}$$

Also, since

$$u_e^2=\bar{u}_e^2+\bar{v}_e^2$$

$$\bar{v}_e=\bar{v}_\infty=\text{Constant}$$

and (for equal increments in p and t)

$$ds=\frac{u_e}{\bar{u}_e}d\bar{x} \tag{69}$$

Then

$$\frac{du_e}{ds}=\left(\frac{\bar{u}_e}{u_e}\right)^2\frac{d\bar{u}_e}{d\bar{x}} \tag{70}$$

Use of these results in the general equation for β as given by equation (52) gives the expression

$$\beta=\frac{2\dfrac{d\bar{u}_e}{d\bar{x}}}{\dfrac{p_e}{p_o}t_e u_e^2}\left[\int_{\bar{x}_o}^{\bar{x}}\frac{p_e}{p_o}\bar{u}_e d\bar{x}+\left(\frac{u_e^2 t_e\beta}{2\dfrac{d\bar{u}_e}{d\bar{x}}}\right)_{\bar{x}_o}\right] \tag{71a}$$

In the vicinity of the stagnation line on a yawed cylinder the parameter β must be a constant since all boundary-layer profiles are similar there. Equation (34) may then be integrated to yield

$$\left(\frac{u_e}{\sqrt{t_e}}\right)_s=A(\xi-\bar{\xi})^{\beta_s/2}$$

where A and $\bar{\xi}$ are also constants. It follows that as $\bar{x}\to 0$, $\beta_s\to 0$ simultaneously since $u_e\to\bar{v}_e$. Equation (71a) may then be written as

$$\beta=\frac{2\dfrac{d\bar{u}_e}{d\bar{x}}}{\dfrac{p_e}{p_s}t_e u_e^2}\int_{\bar{x}_o}^{\bar{x}}\frac{p_e}{p_s}\bar{u}_e d\bar{x} \tag{71b}$$

where $\bar{x}_o$ is arbitrarily small, but $\bar{x}_o=0$ is excluded because from equation (69) $s=-\infty$ when $\bar{x}=0$. Comparison of equations (71b) with the corresponding expression for $\bar{\beta}$ from reference 9

$$\bar{\beta}=\frac{2\dfrac{d\bar{u}_e}{d\bar{x}}}{\dfrac{p_e}{p_s}\lambda t_e\bar{u}_e^2}\int_0^{\bar{x}}\frac{p_e}{p_s}\bar{u}_e d\bar{x} \tag{72}$$

shows that for small values of $\bar{x}_o$ and $\bar{x}\gg\bar{x}_o$

$$\beta=\lambda\left(\frac{\bar{u}_e}{u_e}\right)^2\bar{\beta}=\frac{1-\lambda t_e}{1-t_e}\bar{\beta} \tag{73}$$

The parameter β^* is written in terms of $\bar{\beta}$ and $\bar{u}_e$ by first noting that on the yawed cylinder

$$\frac{1}{G}\frac{dG}{ds}=\frac{1}{\bar{\beta}}\left(\frac{\bar{u}_e}{\bar{u}_e}\right)^2\frac{d}{ds}\left[\bar{\beta}\left(\frac{\bar{u}_e}{u_e}\right)^2\right] \tag{74}$$

which is obtained by substitution of equations (53), (67), and (71) into equation (47) where from figure 6(b)

$$\frac{\partial p/\partial n}{\partial p/\partial s}=-\text{ctn}\,\alpha_e=-\frac{\bar{v}_e}{\bar{u}_e}=-\sqrt{\frac{\lambda-1}{1-\lambda t_e}} \tag{75}$$

(The quantities λ, $\bar{v}_e$, $\Delta\bar{y}$, and Δy are all constants.) Substituting equation (72) into equation (50) then gives

$$\beta^*=\lambda t_e\left[2\bar{\beta}\frac{\lambda-1}{\lambda-\lambda t_e}+\frac{\dfrac{d\bar{\beta}}{d\bar{x}}}{\dfrac{1}{\bar{u}_e}\dfrac{d\bar{u}_e}{d\bar{x}}}\right] \tag{76}$$

From equations (19) and (34) the independent variable η may be written as

$$\eta=\left(\frac{\dfrac{du_e}{ds}}{\beta t_e\rho_w\mu_w}\right)^{1/2}\int_0^z\rho dz$$

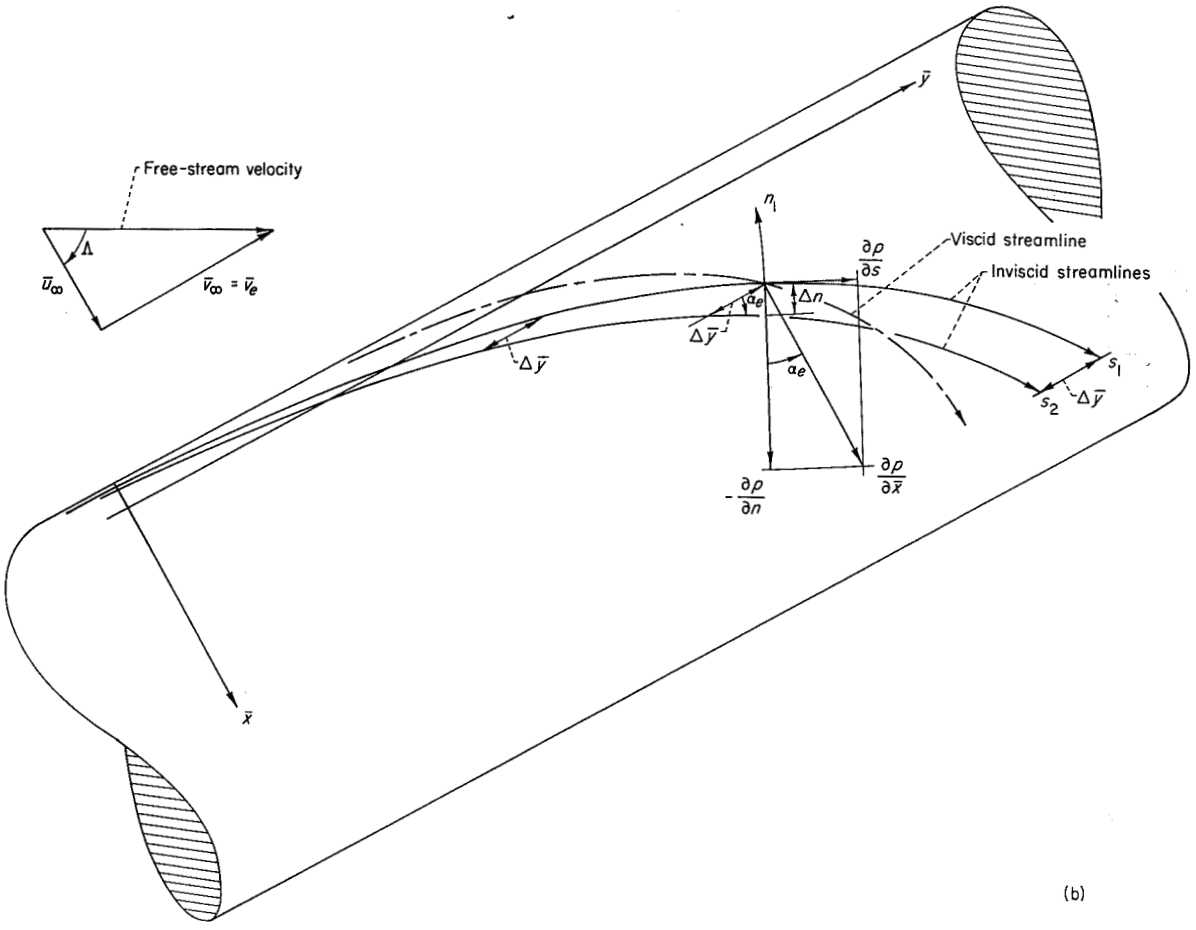

(b) Pressure-gradient components and normal distance between steamlines.

FIGURE 6.—Concluded.

or from equations (70) and (73)

$$\eta=\left(\frac{1}{\lambda t_e}\frac{\frac{d\bar{u}_e}{d\bar{s}}}{\bar{\beta}\rho_w\mu_w}\right)^{1/2}\int_0^z \rho dz$$

Comparison of this equation with the corresponding one for $\bar{\eta}$ from reference 9 shows that

$$\eta=\bar{\eta} \tag{77}$$

The skin-friction components from the exact local similarity method (eqs. (64) and 65)) are then proportional to the following derivatives:

$$\left(\frac{v}{u_e}\right)_w'=-\frac{\lambda-1}{\lambda-\lambda t_e}\sqrt{\frac{1-\lambda t_e}{\lambda-1}}\,(\bar{f}_w''-\bar{g}_w') \tag{78}$$

$$\left(\frac{u}{u_e}\right)_w'=\frac{\lambda-1}{\lambda-\lambda t_e}\,\bar{g}_w'+\frac{1-\lambda t_e}{\lambda-\lambda t_e}\bar{f}_w'' \tag{79}$$

For the assumption of small cross flow, these components are obtained from equations (66) and (67) as

$$\left(\frac{v}{u_e}\right)_w'=\bar{\beta}\frac{\lambda-1}{1-t_e}\sqrt{\frac{1-\lambda t_e}{\lambda-1}}\,V_w' \tag{80}$$

$$\left(\frac{u}{u_e}\right)_w'=f_w'' \tag{81}$$

where equation (66) has been written in the form

$$\frac{v}{u_e}=\frac{\lambda-1}{1-t_e}\sqrt{\frac{1-\lambda t_e}{\lambda-1}}\,\bar{\beta}V \tag{82}$$

by utilization of equations (73) and (75). Equation (82) shows that the direction of v (as determined by its sign) with respect to the positive n direction is negative for positive $\bar{\beta}$ and vice versa since V is always negative. This result is

consistent with equations (48) and (62) and indicates that the assumption of local similarity requires that v change direction when $\bar{\beta}$ goes through 0.

SMALL-CROSS-FLOW CRITERIA

In order to properly assess the comparison of small-cross-flow theory with exact theory on the yawed infinite cylinder, it is desirable to know when the limitation for small cross flow as given by inequality (46) is exceeded. This inequality can be evaluated for the yawed cylinder by substitution of equations (73) and (75) into equation (49). The result is

$$\left(\frac{v}{u}\right)_{max}=\lambda\left(\frac{\bar{u}_e}{u_e}\right)^2\frac{\bar{v}_e}{\bar{u}_e}\bar{\beta}\frac{V'_w}{f''_w}=\frac{\lambda-1}{1-t_e}\left(\frac{1-\lambda t_e}{\lambda-1}\right)^{1/2}\bar{\beta}\frac{V'_w}{f''_w} \tag{83}$$

HEAT TRANSFER

A general expression for the heat-transfer rate at the wall on a three-dimensional body with small cross flow is

$$q_w=\frac{H_e(1-t_w)}{(N_{Pr})_w}\sqrt{\frac{\rho_w\mu_w}{\beta t_e}\frac{du_e}{ds}}\,(1+F_w)\theta'_w \tag{84}$$

which is obtained by application of the assumption of small cross flow to the results of reference 9. That is, in reference 9, x is replaced by s, $t_s=1$, and $r^j=\Delta n$. Then, since from equations (70) and (73)

$$\frac{1}{\bar{\beta}}\frac{du_e}{ds}=\frac{1}{\bar{\beta}}\frac{d\bar{u}_e}{d\bar{x}} \tag{85}$$

equation (84) becomes

$$q_w=\frac{H_e(1-t_w)}{(N_{Pr})_w}\sqrt{\frac{\rho_w\mu_w}{\bar{\beta}}\frac{1}{\lambda t_e}\frac{d\bar{u}_e}{d\bar{x}}}\,(1+F_w)\theta'_w \tag{86}$$

The corresponding exact expression for the yawed cylinder (ref. 9) is

$$\bar{q}_w=\frac{H_e(1-t_w)}{(N_{Pr})_w}\sqrt{\frac{1}{\lambda t_e}\frac{\rho_w\mu_w}{\bar{\beta}}\frac{d\bar{u}_e}{d\bar{x}}}\,(1+F_w)\bar{\theta}'_w$$

hence,

$$\frac{q_w}{\bar{q}_w}=\frac{\theta'_w}{\bar{\theta}'_w} \tag{87}$$

Stagnation region.—In the stagnation region $\beta=0$ and $\theta'_w=0.4696$ (the value for $N_{Pr}=\varphi=1$) independent of t_w; whereas, $\bar{\beta}=1.0$ and $\bar{\theta}'_w$ depends on λ and t_w as given in reference 9. The resulting values of $(q_w/\bar{q}_w)_s$ are plotted against λ in figure 7 for $t_w=0$, 0.5, and 1.0. For small values of t_w and values of λ near 1.0, the small-cross-flow theory predicts heating rates that would be too small by 10 to 15 percent as already shown in reference 6. As λ and t_w are increased the errors increase and become as large as 50 percent in spite of the fact that the cross flow approaches zero in the stagnation region. The small-cross-flow criteria also approach zero as shown by equation (83) for $t_e\to 1/\lambda$. These results indicate that even though the cross-flow velocity is small, the assumption of small cross flow should not be used for prediction of the level of heating at or near the stagnation line of a yawed cylinder.

The validity of equation (86) in the stagnation region is doubtful since equation (85) is correct only for $\bar{x}\gg\bar{x}_o$. If the stagnation region is defined by the conditions

$$p_e\approx p_s$$

$$\frac{d\bar{u}_e}{d\bar{x}}=c$$

$$u_e\approx\bar{v}_e$$

then equation (71b) can be integrated to yield

$$\left(\frac{1}{\beta t_e}\frac{du_e}{ds}\right)_s=\left[\frac{c}{\left(\frac{\bar{x}}{\bar{x}_o}\right)^2-1}\right]_s$$

where equation (70) has been used for the velocity gradient. From equation (69)

$$\left(\frac{\bar{x}}{\bar{x}_o}\right)_s=\left[e^{\frac{c}{\bar{v}_e}(s-s_0)}\right]_s$$

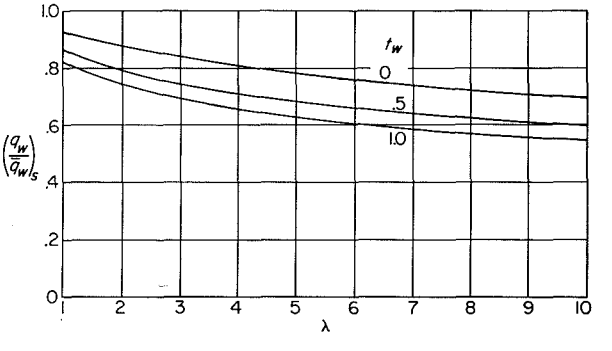

FIGURE 7.—Ratio of heat-transfer rate or spanwise shear in the stagnation region of a yawed cylinder. $N_{Pr}=\varphi=1$.

so that in the stagnation region equation (84) becomes

$$q_{w,s}=H_e(1-t_w)\frac{1+F_w}{(N_{Pr})_w}\left[\rho_w\mu_w\frac{c}{e^{\frac{2c(s-s_o)}{\bar{v}_e}}-1}\right]^{1/2}\theta'_{w,\beta=0}$$

When the quantity $\frac{2c(s-s_o)}{\bar{v}_e}$ is small, this expression for $q_{w,s}$ reduces to

$$q_{w,s}=H_e(1-t_w)\frac{1+F_w}{(N_{Pr})_w}\left[\frac{\rho_w\mu_w\bar{v}_e}{2(s-s_o)}\right]^{1/2}\theta'_{w,\beta=0}$$

which is exactly the result that would be obtained from the similarity theory for a flat plate with external velocity $\bar{v}_e$ and the leading edge at s_o. Thus, the small-cross-flow theory predicts a heating level in the stagnation region that varies with distance along a streamline in essentially the same way as on a flat plate. Since this variation is incorrect from physical considerations (as well as from the exact solution), the conclusion is that the small-cross-flow theory must be used with caution in the stagnation region of a yawed infinite cylinder. If equation (86) is used in the stagnation region, the incorrect dependence of heating on a length does not appear.

Distribution.—The difficulty in the stagnation region of the cylinder can be avoided if the small-cross-flow theory is used only for computing the ratio of local heating to stagnation heating. The level of heating is then established from the appropriate stagnation-line solutions such as those of reference 11. As mentioned previously, this is the recommended procedure for application of the small-cross-flow theory to any arbitrary three-dimensional body for which appropriate stagnation-flow solutions are available in reference 10.

Substitution of equation (85) into equation (57) gives the heat-transfer distribution on a yawed infinite cylinder as

$$\frac{q_w}{q_{w,s}}\frac{(t_{aw}-t_w)_s}{t_{aw}-t_w}=\left[\frac{p_e}{p_s}\frac{1}{t_e\lambda\bar{\beta}}\frac{\frac{d\bar{u}_e}{d\bar{x}}}{\left(\frac{d\bar{u}_e}{d\bar{x}}\right)_s}\right]^{1/2}\frac{1+P\beta^N}{Q+R\beta^N}Q_s \tag{88}$$

since $\bar{\beta}_s=1.0$ and $\beta_s=0$. The corresponding exact expression from reference 9 is

$$\frac{\bar{q}_w}{\bar{q}_{w,s}}\frac{(t_{aw}-t_w)_s}{t_{aw}-t_w}=\left[\frac{p_e}{p_s}\frac{1}{t_e\lambda\bar{\beta}}\frac{\frac{d\bar{u}_e}{d\bar{x}}}{\left(\frac{d\bar{u}_e}{d\bar{x}}\right)_s}\right]^{1/2}\frac{1+P\bar{\beta}^N}{Q+R\bar{\beta}^N} \tag{89}$$

where P, Q, R, and N are functions of both t_w and t_s. (See ref. 9.) Hence, the ratio of the heating (or heat-transfer coefficient) distribution as obtained from small-cross-flow theory to the exact value is

$$\frac{q_w}{\bar{q}_w}=\frac{\left(Q_s\frac{1+P\beta^N}{Q+R\beta^N}\right)_{t_s=1.0}}{\left(\frac{1+P\bar{\beta}^N}{Q+R\bar{\beta}^N}\right)_{t_s\neq1.0}} \tag{90}$$

where the assumption is made that

$$q_{w,s}=\bar{q}_{w,s}$$

CIRCULAR CYLINDER IN SUPERSONIC FLOW

The experimental pressure distribution p_e/p_s on a circular cylinder is essentially independent of yaw angle and Mach number when the normal Mach number is greater than about 2 (as indicated in ref. 9). For a perfect gas, $\bar{\beta}$ as computed from equation (72) is then also independent of yaw angle and Mach number since for this case

$$\lambda t_e=1-\frac{\bar{u}_e^2}{2h_s}=\left(\frac{p_e}{p_s}\right)^{\frac{\gamma-1}{\gamma}}$$

where the flow at the edge of the boundary layer is assumed isentropic.

Similarity parameters.—The pressure distribution on a circular cylinder from reference 9 was used in equation (72) to compute $\bar{\beta}$. The resulting curve, which is then independent of Mach number and yaw angle for normal Mach numbers greater than 2, is shown in figure 8(a). Also shown in figure 8(a) are corresponding curves for β computed from equation (73) for several values of λ. In figure 8(b) the variation of β^* as computed from equation (76) is shown for several values of λ.

Small-cross-flow criteria.—Values of $(v/u)_{max}$ were computed for the circular cylinder from equation (83), and the square of this quantity is plotted against $\bar{x}/r$ in figure 9. This figure indicates that the limitation of the inequality (46)

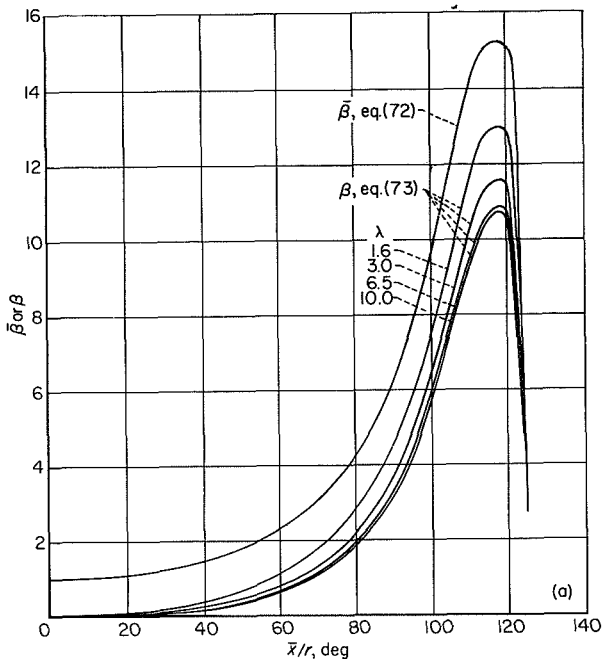

(a) $\bar{\beta}$ and β.

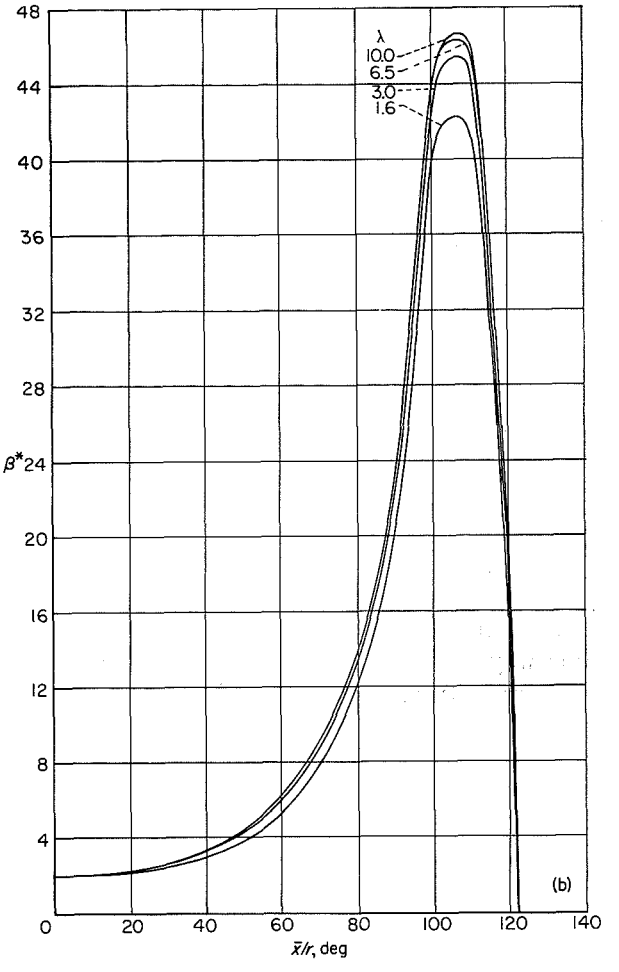

(b) β^*, equation (76).

FIGURE 8.—Local similarity parameters on a circular cylinder for various values of the yaw parameter λ.

is exceeded except for small values of t_w and λ near 1.0. (The stagnation line and immediate vicinity should be excluded from consideration in accordance with previous discussion.) Hence, the assumption of small cross flow would not be expected to yield accurate predictions of skin friction and heat transfer when t_w and λ are large. These rather arbitrary limits will be determined more precisely by detailed comparisons of results from the theories in the following sections.

Velocity profiles.—Cross-flow and streamwise velocity profiles have been computed from equations (64), (65), (67), and (82) at several $\bar{x}$ stations on a circular cylinder with t_w=0.5 and λ=3. These values for t_w and λ are representative of wind-tunnel conditions at a Mach number of 6.2 and a sweep angle of 60°. In equations (64) and (65) the values of $\bar{f}'$ and $\bar{g}$ were obtained from similar solutions to the boundary-layer equations for the yawed infinite cylinder (refs. 9 and 11) with $\bar{\beta}$ from figure 8(a) as the parameter. In equation (67) f' is a function of β (fig. 8(a)), and in equation (82) V was taken from the numerical solutions of equation (32) and is a function of both β and β^*. (Since the numerical solutions were limited to the values of β and β^* in table I, it was not generally possible to obtain exact correspondence of these two parameters as required by figure 8.) The resulting profiles are shown in figure 10 where the values of $\bar{\beta}$ and β are at the correct $\bar{x}/r$ from figure 8 but the given value of β^* would be at a slightly different $\bar{x}/r$.

Over the forward portion of the cylinder (figs. 10(b) and 10(c)) the cross-flow profiles from equation (82) are in good agreement with the corresponding exact profiles from equation (64). However, the streamwise profiles from equation (67) are not in such good agreement with the exact profiles from equation (65) in this region (figs. 10(a) to 10(c)). Further back on the cylinder (figs. 10(d) and 10(e)) the converse appears to be true in that the cross-flow profiles differ considerably whereas the streamwise profiles are nearly the

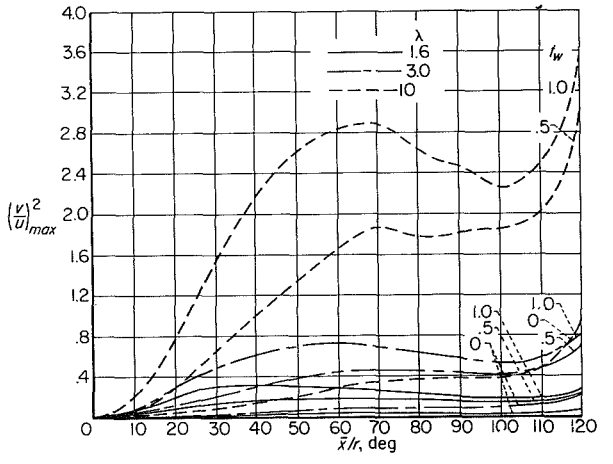

FIGURE 9.—Criteria for small cross flow on a yawed circular cylinder for various values of λ and t_w.

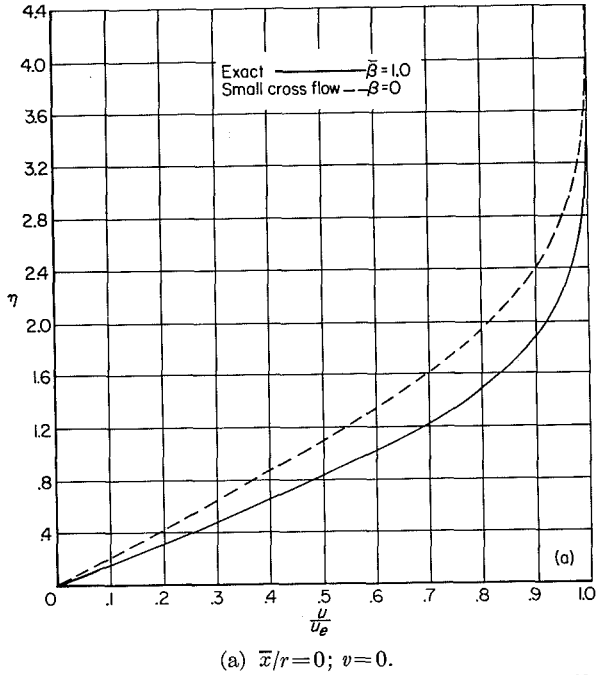

(a) $\bar{x}/r=0$; $v=0$.

FIGURE 10.—Cross-flow and streamwise velocity profiles on a circular cylinder for $\lambda=3$ and $t_w=0.5$. Equations (64) and (65) were used for the exact profiles, and equations (67) and (82), for the profiles by small-cross-flow theory.

same. Since the similar solutions are available only at discrete values of the parameters $\bar{\beta}$, β, and β^*, the comparable profiles could not usually be obtained at exactly the same station on the cylinder or for the correct value of β^*. Nevertheless, the small-cross-flow theory generally provides a reasonable approximation to the velocity profiles even though $(v/u)^2_{max} \approx 0.5$ from figure 9.

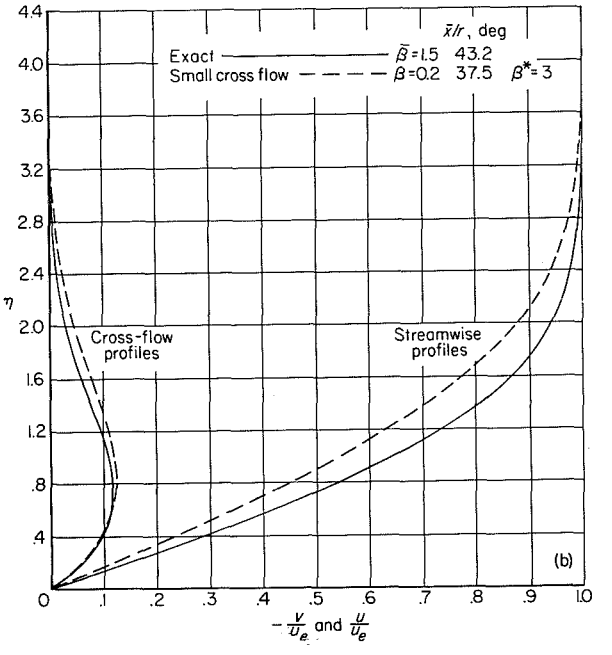

(b) $\bar{x}/r \approx 40°$.

FIGURE 10.—Continued.

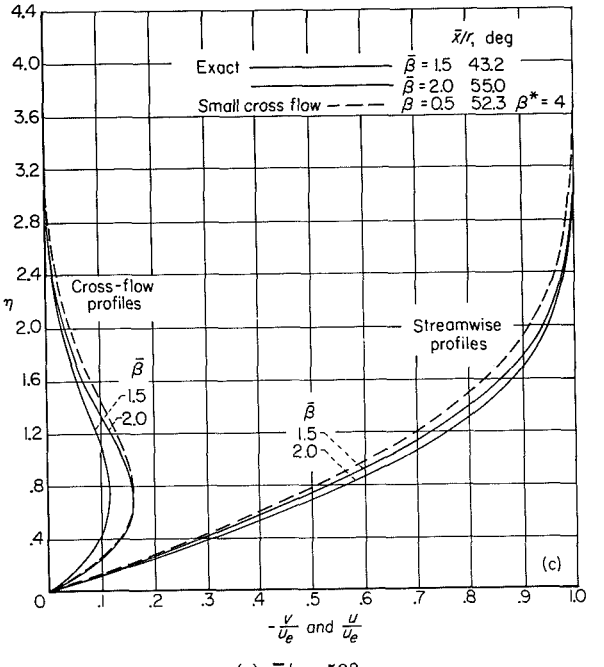

(c) $\bar{x}/r \approx 50°$.

FIGURE 10.—Continued.

Skin friction.—The difficulty in obtaining velocity profiles at the same station can be avoided in a comparison of skin friction since interpolation formulas or plots for $\bar{f}_w''$, $\bar{g}_w'$, and f_w' as functions of $\bar{\beta}$ and β may be used with figure 8(a) supplying

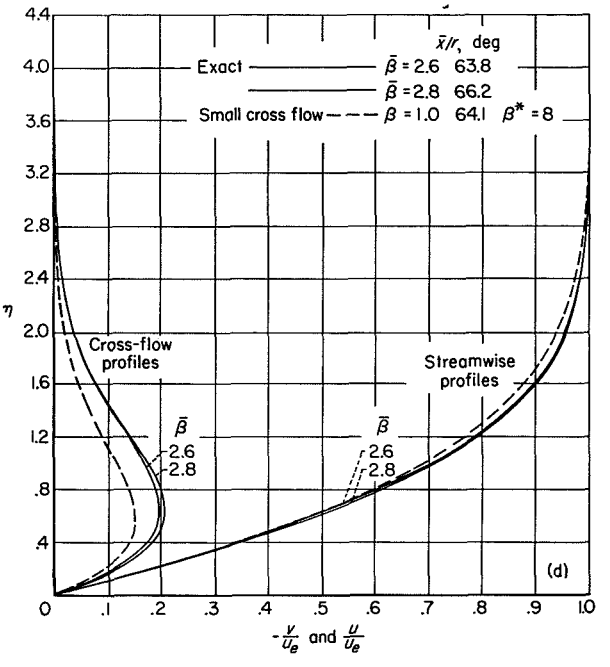

(d) $\bar{x}/r \approx 65°$.

FIGURE 10.—Continued.

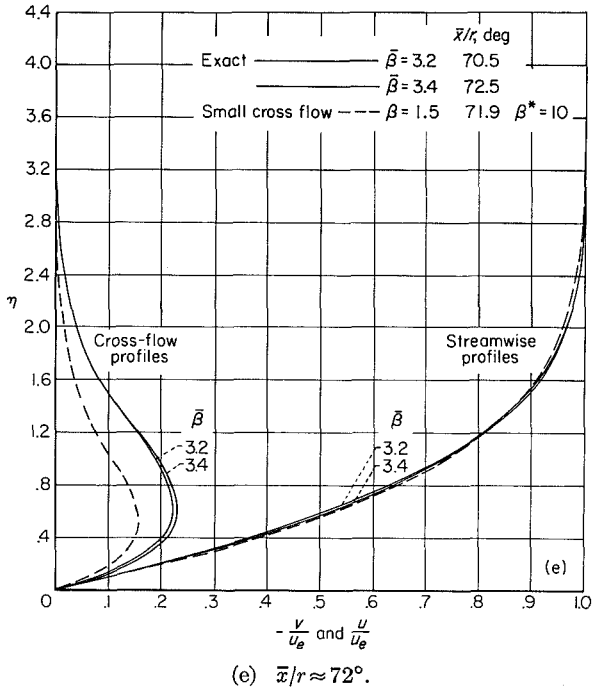

(e) $\bar{x}/r \approx 72°$.

FIGURE 10.—Concluded.

the corresponding functional dependence on $\bar{x}/r$. The skin-friction parameters were computed in this manner from equations (78) to (81) where the approximate solution of equation (32) was used to evaluate V'_w (eqs. (41) and (42) or appendix) for corresponding values of β and β^* as given in figure 8. The results are shown in figure 11 for $t_w=0$ and 0.5 with $\lambda=3$ and 10.

The same general trends are evident in figure 11 as already noted in figure 10. That is, the exact and small-cross-flow values (figs. 11(a) and (b)) tend to agree better over the forward portion of the cylinder ($\theta \lessapprox 60°$) whereas the streamwise parameters (figs. 11 (c) and (d)) are in better agreement over the aft portion of the cylinder ($\theta \gtrapprox 60°$). The cross-flow skin friction for $\lambda=10$ and $t_w=0.5$ (fig. 11(b)) is an exception to the previous statement since for this case the agreement improves for increasing $\bar{x}/r$ and is surprisingly good in view of the large cross flow present. (From fig. 9 $(v/u)^2_{max} \approx 2.0$.) On the aft portion of the cylinder

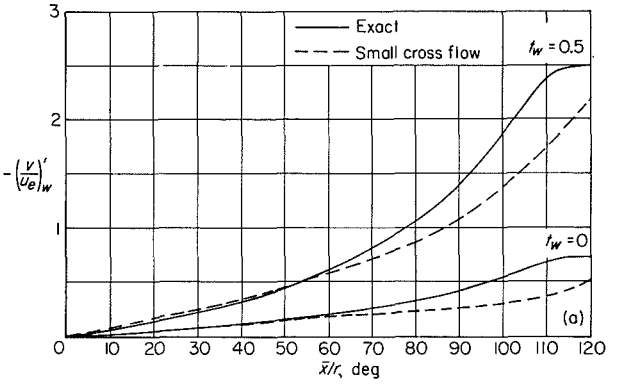

(a) Cross-flow parameter for $\lambda=3$.

FIGURE 11.—Skin-friction parameters on a circular cylinder for $t_w=0$ and 0.5. $N_{Pr}=\varphi=1$.

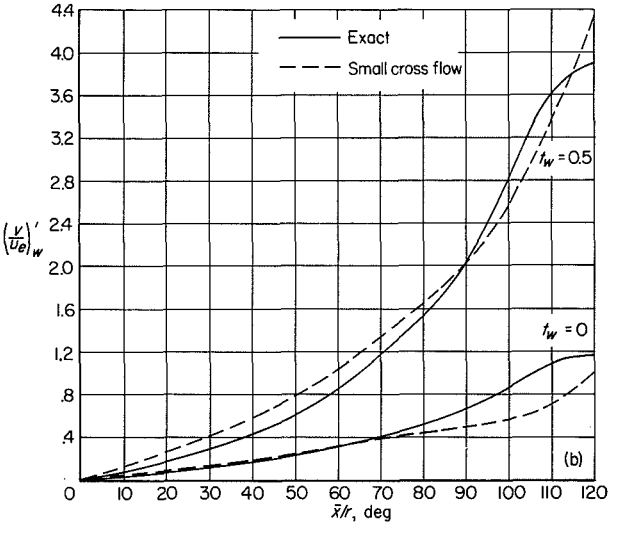

(b) Cross-flow parameter for $\lambda=10$.

FIGURE 11.—Continued.

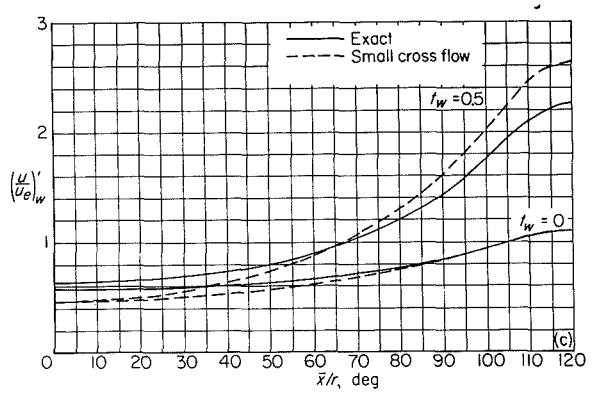

(c) Streamwise parameter for $\lambda=3$.

FIGURE 11.—Continued.

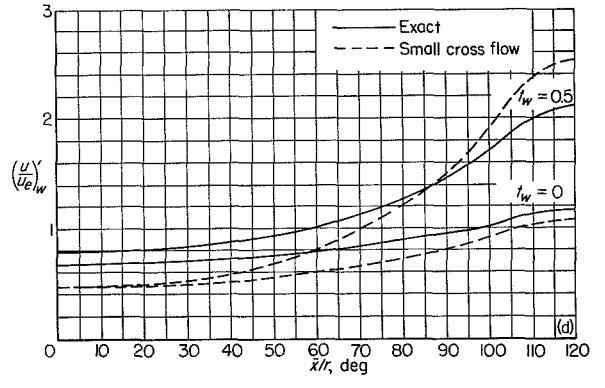

(d) Streamwise parameter for $\lambda=10$.

FIGURE 11.—Concluded.

the present theory predicts the cross-flow skin friction better for $t_w=0.5$ than for $t_w=0$. This result is also contrary to the criteria of figure 9 which would indicate that better predictions should always be obtained for $t_w=0$.

The values of the streamwise skin-friction parameter from the small-cross-flow theory are always in better agreement with the exact values when $t_w=0$. (See figs. 11(c) and 11(d).) For $\lambda=10$ and $t_w=0.5$ (fig. 11(d)), the shear parameter is about 40 percent too low for $\theta \lessapprox 30°$ as would be expected from figure 7; however, for $\theta \gtrapprox 50°$ the errors are smaller where $(v/u)^2_{max}$ becomes larger. Apparently both the cross-flow and streamwise skin frictions are predicted with fair accuracy for $t_w=0.5$ on the aft portion of the cylinder where $(v/u)^2_{max} \approx 2.0$.

Heat-transfer distribution.—The normalized heat-transfer distribution was calculated from equation (90) with use of the values of P, Q, R, and N from reference 9 and β and $\overline{\beta}$ from figure 8(a) for the circular cylinder. The results are plotted in figure 12 which shows that the small-cross-flow theory predicts heat-transfer distribution to within about 15 percent of the correct value for t_w from 0 to 1 and for λ up to 10. From figure 9, the values of $(v/u)^2_{max}$ may become as large as 4 for these conditions. These results, therefore, indicate that the heat-transfer distribution as computed by the small-cross-flow theory is insensitive to the magnitude of the cross flow present on a yawed cylinder. Whether the cross flow will have such a small effect on other more general three-dimensional shapes is not known. Such a result would seem likely, however, with the explanation based on the hypothesis that the local profile shapes of the total stagnation enthalpy are affected only slightly by cross-flow pressure gradients. This hypothesis would then extend the theory of reference 9 for the heat-transfer distribution on a body of revolution to an arbitrary three-dimensional shape. In the latter case, the theory of reference 9 is modified so as to properly account for the streamwise pressure gradient by calculation of the heating distribution along the inviscid streamlines.

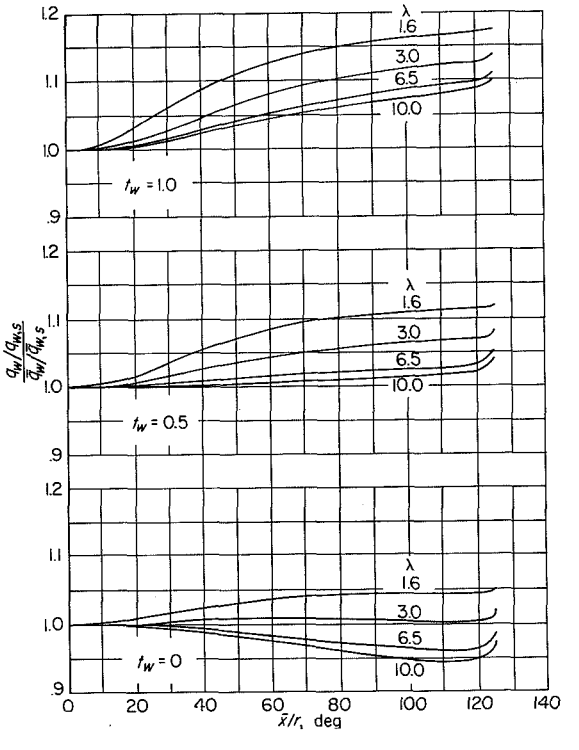

FIGURE 12.—Ratio of exact heat-transfer distribution to small-cross-flow heat-transfer distribution on a circular cylinder at yaw.

CONCLUDING REMARKS

With the use of a streamline coordinate system and the assumption of small cross flow, the continuity, energy, and streamwise momentum equations for the boundary layer on an arbitrary three-dimensional body are reduced to the form taken by these equations for an axisymmetric body. The local radius of the body of revolution in the latter equations is replaced by a metric coefficient in the streamline coordinate system. The skin friction and heat transfer are then calculated along the inviscid streamlines by a local similarity method originally derived for a body of revolution but here modified to account for the different coordinate system.

A similarity-type transformation is applied to the cross-flow momentum equation which is then reduced to an ordinary differential equation by the assumption of similarity in the cross-flow velocity function. The physical cross-flow velocity is proportional to the product of this cross-flow velocity function and the ratio of the crosswise pressure gradient to the streamwise pressure gradient. Besides the usual similarity pressure-gradient parameter, the cross-flow velocity function depends also on a new similarity parameter which is partly determined by the streamwise derivative of the pressure-gradient ratio. Suitable equations are derived for computation of these parameters.

General criteria which are used to define the limiting conditions for valid application of the assumption of small cross flow are evaluated from solutions of the reduced cross-flow momentum equation. In order to apply the criteria to any particular case, the pressure-gradient ratio must be known along the inviscid streamlines.

As an illustrative example, the small-cross-flow theory is used to compute the velocity profiles, skin friction, and heating distribution on a yawed circular cylinder. These results are compared to the corresponding "exact" values as obtained from local similarity solutions already available for the yawed infinite cylinder. These comparisons indicate that the small-cross-flow theory provides reasonable approximations to the velocity profiles and skin friction even when the cross-flow velocity is much larger than specified by the limiting criteria. The heating distributions on the yawed cylinder were predicted to within 15 percent of the correct values for a large range of wall temperature, Mach number, and yaw angle. Since the small-cross-flow criteria were again considerably exceeded for these conditions, it seems likely that the assumption of small cross flow may be applicable (particularly for the computation of heating distributions) to a larger range of body shapes, wall temperatures, and stream conditions than previously considered possible.

LANGLEY RESEARCH CENTER,
NATIONAL AERONAUTICS AND SPACE ADMINISTRATION,
LANGLEY FIELD, VA., *April 6, 1961.*

APPENDIX

APPROXIMATE INTEGRAL SOLUTION OF CROSS-FLOW MOMENTUM EQUATION

The cross-flow momentum equation (eq. (32) in text) is

$$V''+fV'-\beta^* f'V=(1-t_w)\theta+t_w-f'^2 \quad \text{(A1)}$$

with boundary conditions

$$V(0)=V(\infty)=0 \quad \text{(A2)}$$

The functions f and θ are known from solutions of equation (30) and (31) and their boundary conditions are

$$\left.\begin{aligned} f(0)=f'(0)=\theta(0)=0 \\ f'(\infty)=\theta(\infty)=1 \end{aligned}\right\} \quad \text{(A3)}$$

The cross-flow velocity function is assumed to be a sixth-degree polynomial of the form

$$V=a_1\eta+a_2\eta^2+a_3\eta^3+a_4\eta^4+a_5\eta^5+a_6\eta^6 \quad \text{(A4)}$$

where from equations (A1), (A2), and (A3)

$$a_2=\frac{1}{2}V''_w=\frac{1}{2}t_w \quad \text{(A5)}$$

$$a_3=\frac{1}{6}V'''_w=\frac{1}{6}(1-t_w)\theta'_w \quad \text{(A6)}$$

The four remaining coefficients are determined from equation (A4) by specifying that

$$V(\eta_e)=V'(\eta_e)=V''(\eta_e)=V'''(\eta_e)=0 \quad \text{(A7)}$$

which after the use of equations (A5) and (A6) yields

$$a_1=V'_w=-\frac{1}{5}t_w\eta_e-\frac{1}{60}(1-t_w)\theta'_w\eta_e^2 \quad \text{(A8)}$$

$$\left.\begin{aligned} a_4&=-t_w\frac{1}{\eta_e^2}-\frac{1}{3}(1-t_w)\theta'_w\frac{1}{\eta_e} \\ a_5&=t_w\frac{1}{\eta_e^3}+\frac{1}{4}(1-t_w)\theta'_w\frac{1}{\eta_e^2} \\ a_6&=-\frac{3}{10}t_w\frac{1}{\eta_e^4}-\frac{1}{15}(1-t_w)\theta'_w\frac{1}{\eta_e^3} \end{aligned}\right\} \quad \text{(A9)}$$

Since there are still two unknowns V'_w and η_e another independent equation is required. This equation is obtained by integration of equation (A1) from $\eta=0$ to ∞ with the boundary conditions of equations (A2) and (A3) and $V'(\infty)=0$. The result is

$$V'_w=-(\beta^*+1)\int_0^\infty f'Vd\eta-\int_0^\infty[(1-t_w)\theta+t_w-f'^2]d\eta$$

or substituting equation (40b) for the last term and noting that $V(\eta_e)=0$ gives

$$V'_w=-(\beta^*+1)\int_0^{\eta_e}f'Vd\eta+\frac{1}{\beta}(\theta^*_{tr}-f''_w) \quad \text{(A10)}$$

The integral term is evaluated by assuming a fifth-degree profile for the product function $f'V$. That is,

$$f'V=b_1\eta+b_2\eta^2+b_3\eta^3+b_4\eta^4+b_5\eta^5 \quad \text{(A11)}$$

Differentiation of equation (A11) and application of the boundary conditions of equations (A2) and (A3) then gives

$$\left.\begin{aligned} b_1&=0 \\ b_2&=f''_wV'_w \end{aligned}\right\} \quad \text{(A12)}$$

The remaining three coefficients are evaluated by use of the conditions of equation (A7) in the derivatives of equation (A11) which results in

$$\left.\begin{aligned} b_3&=-3f''_w V'_w \frac{1}{\eta_e} \\ b_4&=3f''_w V'_w \frac{1}{\eta_e^2} \\ b_5&=-f''_w V'_w \frac{1}{\eta_e^3} \end{aligned}\right\} \tag{A13}$$

Substituting equations (A11), (A12), and (A13) in equation (A10) and solving for V'_w gives the expression

$$V'_w=\frac{\frac{1}{\beta}(\theta^*_{tr}-f''_w)}{1+\frac{\beta^*+1}{60}f''_w\eta_e^3} \tag{A14}$$

Simultaneous solution of equations (A8) and (A14) for V'_w and η_e then provides all quantities required to evaluate V.

REFERENCES

1. Hayes, Wallace D.: The Three-Dimensional Boundary Layer. NAVORD Rep. 1313 (NOTS 384), U.S. Naval Ord. Test Station, Inyokern (China Lake, Calif.), May 9, 1951.
2. Eichelbrenner, E.-A., and Oudart, A.: Méthode de Calcul de la Couche Limite Tridimensionnelle. Application a un Corps Fuselé Incliné sur le Vent. O.N.E.R.A. Pub. No. 76, 1955.
3. Cooke, J. C., and Hall, M. G.: Boundary Layers in Three Dimensions. Rep. No. Aero.2635, British R.A.E., Feb. 1960.
4. Hall, M. G.: On the Momentum Integral Equations for Three-Dimensional Laminar Boundary Layers in Incompressible Flow. Rep. ACA–62, Dept. Supply, Australian Aero. Res. Committee, Nov. 1959.
5. Zaat, J. A.: A Simplified Method for the Calculation of Three-Dimensional Laminar Boundary Layers. Rep. F.184, Nationaal Luchtvaartlaboratorium (Amsterdam), Apr. 1956.
6. Vaglio-Laurin, Roberto: Laminar Heat Transfer on Three-Dimensional Blunt Nosed Bodies in Hypersonic Flow. ARS Jour., vol. 29, no. 2, Feb. 1959, pp. 123-129.
7. Lees, Lester: Laminar Heat Transfer Over Blunt-Nosed Bodies at Hypersonic Flight Speeds. Jet Propulsion, vol. 26, no. 4, Apr. 1956, pp. 259–269, 274.
8. Kemp, Nelson H., Rose, Peter H., and Detra, Ralph W.: Laminar Heat Transfer Around Blunt Bodies in Dissociated Air. Jour. Aero/Space Sci., vol. 26, no. 7, July 1959, pp. 421–430.
9. Beckwith, Ivan E., and Cohen, Nathaniel B.: Application of Similar Solutions to Calculation of Laminar Heat Transfer on Bodies With Yaw and Large Pressure Gradient in High-Speed Flow. NASA TN D–625, 1961.
10. Reshotko, Eli: Heat Transfer to a General Three-Dimensional Stagnation Point. Jet Propulsion, vol. 28, no. 1, Jan. 1958, pp. 58–60.
11. Beckwith, Ivan E.: Similar Solutions for the Compressible Boundary Layer on a Yawed Cylinder With Transpiration Cooling. NASA TR R–42, 1959. (Supersedes NACA TN 4345.)
12. Howarth, L.: The Boundary Layer in Three Dimensional Flow.-Part I. Derivation of the Equations for Flow Along a General Curved Surface. Phil. Mag., ser. 7, vol. 42, no. 326, Mar. 1951, pp. 239–243.
13. Cohen, Nathaniel B.: Correlation Formulas and Tables of Density and Some Transport Properties of Equilibrium Dissociating Air for Use in Solutions of the Boundary-Layer Equations. NASA TN D–194, 1960.
14. Cohen, Clarence B., and Reshotko, Eli: Similar Solutions for the Compressible Laminar Boundary Layer With Heat Transfer and Pressure Gradient. NACA Rep. 1293, 1956. (Supersedes NACA TN 3325.)
15. Reshotko, Eli, and Beckwith, Ivan E.: Compressible Laminar Boundary Layer Over a Yawed Infinite Cylinder With Heat Transfer and Arbitrary Prandtl Number. NACA Rep. 1379, 1958. (Supersedes NACA TN 3986.)

U.S. GOVERNMENT PRINTING OFFICE: 1962

NASA TR R-107
National Aeronautics and Space Administration.
SIMILARITY SOLUTIONS FOR SMALL CROSS FLOWS IN LAMINAR COMPRESSIBLE BOUNDARY LAYERS. Ivan E. Beckwith. 1961. i, 26 p. diagrs., tab. GPO price 40 cents. (NASA TECHNICAL REPORT R—107).

The boundary-layer equations for three-dimensional flow have been simplified by the use of a streamline coordinate system and the assumptions of small cross flow and similar profiles. Equations for heat transfer and skin friction for axisymmetric flow are then applicable to three-dimensional flow. Solutions of the cross-flow momentum equation are used to evaluate limiting conditions for the valid assumption of small cross flow. Results from the present method are in good agreement with exact solutions for a yawed cylinder.

(Initial NASA distribution: 1, Aerodynamics, aircraft; 2, Aerodynamics, missiles and space vehicles; 20, Fluid mechanics.)

Copies obtainable from Supt. of Docs., GPO, Washington

I. Beckwith, Ivan E.
II. NASA TR R-107

NASA

NASA TR R-107
National Aeronautics and Space Administration.
SIMILARITY SOLUTIONS FOR SMALL CROSS FLOWS IN LAMINAR COMPRESSIBLE BOUNDARY LAYERS. Ivan E. Beckwith. 1961. i, 26 p. diagrs., tab. GPO price 40 cents. (NASA TECHNICAL REPORT R—107).

The boundary-layer equations for three-dimensional flow have been simplified by the use of a streamline coordinate system and the assumptions of small cross flow and similar profiles. Equations for heat transfer and skin friction for axisymmetric flow are then applicable to three-dimensional flow. Solutions of the cross-flow momentum equation are used to evaluate limiting conditions for the valid assumption of small cross flow. Results from the present method are in good agreement with exact solutions for a yawed cylinder.

(Initial NASA distribution: 1, Aerodynamics, aircraft; 2, Aerodynamics, missiles and space vehicles; 20, Fluid mechanics.)

Copies obtainable from Supt. of Docs., GPO, Washington

I. Beckwith, Ivan E.
II. NASA TR R-107

NASA

NASA TR R-107
National Aeronautics and Space Administration.
SIMILARITY SOLUTIONS FOR SMALL CROSS FLOWS IN LAMINAR COMPRESSIBLE BOUNDARY LAYERS. Ivan E. Beckwith. 1961. i, 26 p. diagrs., tab. GPO price 40 cents. (NASA TECHNICAL REPORT R—107).

The boundary-layer equations for three-dimensional flow have been simplified by the use of a streamline coordinate system and the assumptions of small cross flow and similar profiles. Equations for heat transfer and skin friction for axisymmetric flow are then applicable to three-dimensional flow. Solutions of the cross-flow momentum equation are used to evaluate limiting conditions for the valid assumption of small cross flow. Results from the present method are in good agreement with exact solutions for a yawed cylinder.

(Initial NASA distribution: 1, Aerodynamics, aircraft; 2, Aerodynamics, missiles and space vehicles; 20, Fluid mechanics.)

Copies obtainable from Supt. of Docs., GPO, Washington

I. Beckwith, Ivan E.
II. NASA TR R-107

NASA